Quaternary Science Reviews 70 (2013) 28–47

Contents lists available at SciVerse ScienceDirect

Quaternary Science Reviews

journal homepage: www.elsevier.com/locate/quascirev

Holocene vegetation history and sea level changes in the SE corner of the Caspian Sea: relevance to SW Asia climate

Suzanne A.G. Leroy [a,*], Ata A. Kakroodi [b,1], Salomon Kroonenberg [b], Hamid K. Lahijani [c], Habib Alimohammadian [d], Aman Nigarov [e]

[a] Institute for the Environment, Brunel University, Kingston Lane, Uxbridge, UB8 3PH London, UK
[b] Department of Geotechnology, Delft University of Technology, The Netherlands
[c] Iranian National Institute for Oceanography (INIO), No. 3 Etamadzadeh St, Fatemi Avenue, Tehran 1411813389, Iran
[d] Geological Survey of Iran, Tehran, Iran
[e] Main National Museum of Turkmenistan, Ashgabat, Turkmenistan

ARTICLE INFO

Article history:
Received 16 November 2012
Received in revised form
4 March 2013
Accepted 6 March 2013
Available online 20 April 2013

Keywords:
Pollen
Vegetation
Dinocyst
Sea level
Alborz Mountains
Caspian Sea
Holocene
Asian summer monsoon

ABSTRACT

The palynological investigation of core TM (27.7 m long) taken in a dried out lagoon reveals both Holocene vegetation history in the north-eastern foothills of the Alborz Mountains and past water level changes of the Caspian Sea (CS).

The delay in woodland expansion at the beginning of the Holocene, which is typical of eastern Turkey, the Iranian plateau and recorded in the CS south basin, is only weakly felt as the region is close to glacial refugia of trees.

The succession of the main trees out of their refugia has been established as deciduous *Quercus, Carpinus betulus, Parrotia persica,* and *Fagus orientalis-Pterocarya fraxinifolia*, presenting therefore close affinities to south European interglacials of the Early Pleistocene. This suggests a similarity in climate.

A *Pterocarya* decline is observed after AD 495. The studied region is close to the easternmost tree distribution; this could explain why it has been affected earlier than elsewhere in the northern Alborz and the Caucasus. In addition human activities during the Sasanian Empire and the subsequent drying of the climate contributed to weakening the spread of this tree.

A maximal sea level occurs in the first part of the Holocene from 10.6 to 7.2 cal. ka. It is suggested that the CS levels were significantly influenced by the monsoon precipitations over the western Himalayas (via the Uzboy inflow). This is followed by low levels from 7.2 to 3.5 cal. ka with a minimum at 3.9 cal. ka.

The Neocaspian period should be considered a biozone rather than a chronozone, as the environmental conditions reconstructed from dinocyst assemblages are different in shallow shelf waters and in the deep basins.

1. Introduction

The extent of the Holocene changes in the Caspian Sea (CS) water level is so far poorly known and subject to intense controversies (Rychagov, 1997; Svitoch, 2009). The water level changes of the CS are not synchronous with the global sea level changes, not even in anti-phase. Its widely changing palaeo-hydrography has often more influence than the simple relationship with precipitation over the catchment-sea level change. Since its formation, the CS has at times had an outflow to the Black Sea; at other times it was a closed sea. The number of large rivers flowing to the sea has also fluctuated over time, usually with the Volga River bringing > 80% of the water but at other times it was under the influence of the Amu-Daria (daria means river) and its catchment in the western Himalayas (Leroy et al., 2007) (Fig. 1A).

Most sea level information is typically derived from sedimentological–palaeoecological analyses of outcrops around the middle and the north basins with only a few cores from the deep middle and south basins. During the Lateglacial, the CS had most likely higher than present water levels due to meltwater from the Eurasian ice sheet. This period is termed the Khvalynian in the Russian stratigraphy of the CS. This was followed by a brief but poorly dated very low level, the Mangyshlak. Then the Holocene intermediate levels were reached; this is called the Neocaspian.

* Corresponding author. Tel.: +44 1895 266087; fax: +44 1895 269761.
E-mail address: suzanne.leroy@brunel.ac.uk (S.A.G. Leroy).
[1] Present address: Department of Remote Sensing, Faculty of Geography, University of Tehran, Tehran, Iran.

0277-3791
http://dx.doi.org/10.1016/j.quascirev.2013.03.004

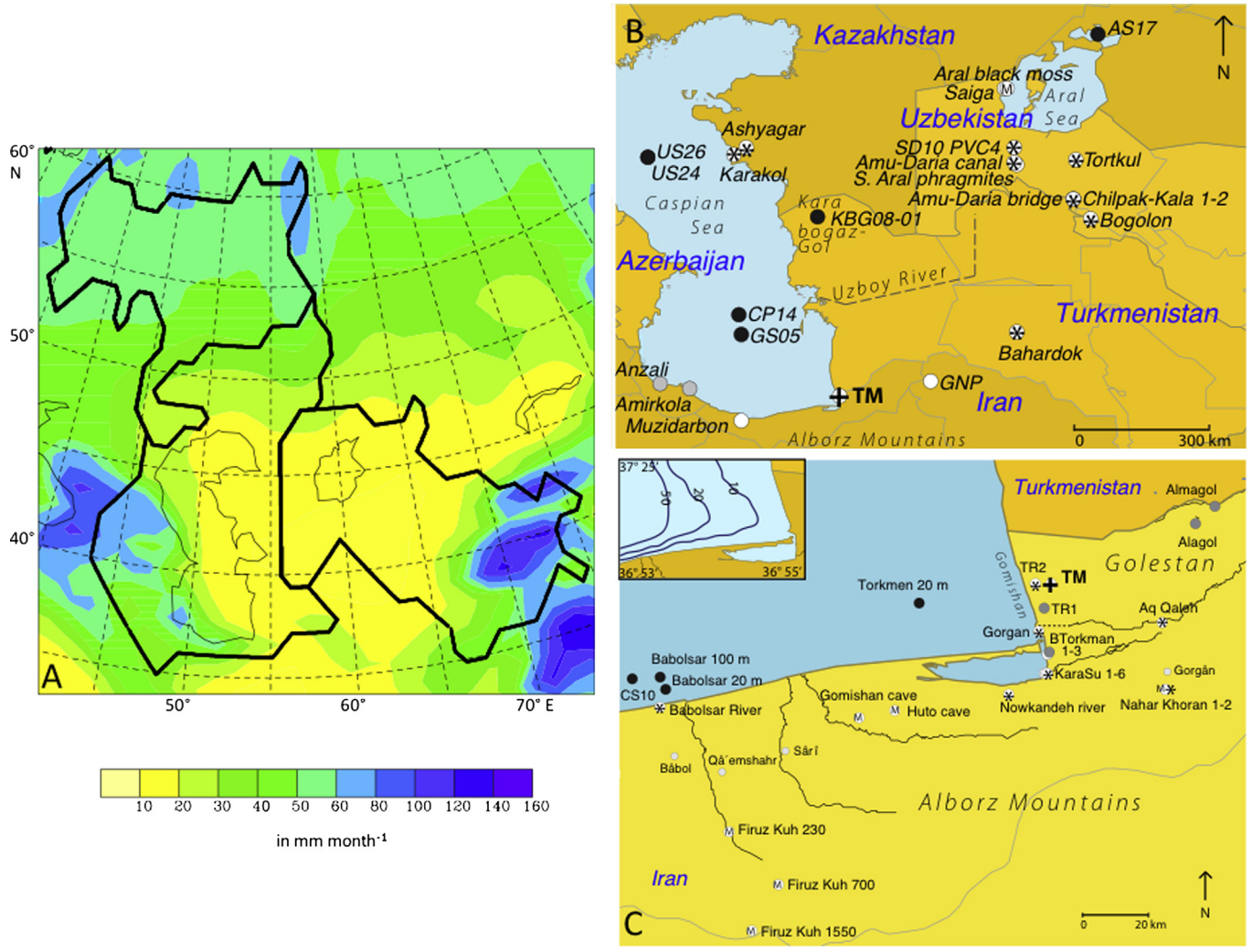

Fig. 1. A: Mean annual precipitations for the area of the Caspian and Aral Sea drainage basins (data from the ECMWF interim reanalysis). Colours are for different mm per month values. Black lines: drainage basin limits. 1B: Location of surface samples in the south-east and east of the Caspian Sea area with river and lagoon names. Black circles for marine sites, grey circles for lagoons, stars on white circles for mud samples, M on white circles for moss polsters and white circles for other sequences cited in the text. 1C: Location of the surface samples and core TM in the south-east corner of the Caspian Sea. Inset showing the shallow shelf in front of the Gomishan coastline, with bathymetric contours for 10, 20 and 50 m. Black circles for marine sites, grey circles for lagoons, stars on white circles for mud samples, and M on white circles for moss polsters. The small light grey circles indicate towns. (For interpretation of the references to colour in this figure legend, the reader is referred to the web version of this article.)

This period may have started anywhere between the beginning of the Holocene and the mid-Holocene according to various authors (Rychagov, 1997; Svitoch, 2009).

The Holocene vegetation history of the CS surroundings is not known. Only short sequences from the south and middle basins have been published, showing a subtle interplay between more or less steppic landscapes (Leroy et al., 2007). In the centre of the Iranian coast, some diagrams covering the last centuries only reveal the existence of a diverse forest (Ramezani et al., 2008; Leroy et al., 2011). However, the probable wide displacement of vegetation belts on the northern flank of the Alborz Mountains, a refugium for some Arcto-Tertiary tree species, is so far totally unknown.

Palynological analyses involving pollen, spores, non-pollen palynomorphs and dinoflagellate cysts (dinocysts) are a powerful tool to reconstruct both terrestrial and aquatic changes. The forest of the south of the CS, i.e. the Hyrcanian forest, is ecologically and palaeo-ecologically interesting as it contains a few endemic species that were widespread in Europe during the Pliocene or even Early and Middle Pleistocene such as *Parrotia persica, Zelkova carpinifolia*, *Pterocarya fraxinifolia* and *Gleditsia caspica* (Leroy and Roiron, 1996; Akhani et al., 2010). It is not clear i) when this forest developed after the Last Glacial Maximum in northern Iran, ii) if there was an early Holocene dry period when Europe had a climatic optimum, and iii) what was the succession of trees, out their glacial refugia.

The dinocysts of the CS contain many forms, species and even some genera that are endemic. They have been described in detail recently in Marret et al. (2004). Although it is possible to identify them using a firm taxonomy, their ecological requirements remain at times poorly known. Notwithstanding that limitation, some past sea levels reconstructions may be attempted using the full range of palynomorphs and comparing these with other proxies, such as sedimentology.

The aims of this investigation are therefore to reconstruct i) the Holocene vegetation history in the foothills of the Alborz Mountains and ii) the Holocene water level changes of the CS from the evidence of a 27.7 m long sediment core (TM) taken in a palaeo-lagoon in the SE corner of the CS.

2. Setting

The CS is an endorheic lake, which is the world's largest lake in terms of both area and volume, extending 35–48° N and 47–55° E

(Fig. 1A and B). Three basins divide the sea, becoming deeper southwards: the northern basin (80,000 km^2) with an average depth of 5–6 m and a maximum depth of 15–20 m; the middle basin (138,000 km^2) with an average depth of 175 m and a maximum depth of 788 m; and the southern basin (168,000 km^2) with an average depth of 325 m and a maximum depth of 1025 m (Leroy et al., 2007). The southern basin holds more than 65% of the CS water. The CS nowadays is fed by several rivers, of which the Volga is by far the most important bringing 80% of its water volume. However the highest volume of sediment comes from the Sefidrud (Iran) and the Kura (Azerbaijan) Rivers (Lahijani et al., 2008). On the Iranian coast, the Gorgan River (240 km long) is the second most important river; it flows east–west just south of the study site, in the SE corner of the CS (Fig. 1). This river has changed its course several times during the last centuries, migrating north–south (Kakroodi et al., 2012).

North of the Gorgan delta in the Gomishan area, the coastal area of the Golestan Province of NE Iran, the coast has known many historical changes in its geomorphology due to rapid sea level changes over the last centuries (Fig. 1C). A large inland lagoon, the Hassan Gholi Bay, was a dominant feature at least until 1890. Further north the lagoon penetrated deeply into the coastal plain, and contained a small delta of the intermittent Atrak River, which is 530 km long and also flows east–west. During sea-level fall between 1929 and 1977, the whole lagoon dried out, the coastline shifted kilometres seaward but with the subsequent CS level (CSL) rise of 1977–1995 a new lagoon formed (Kakroodi et al., 2012).

In the Late Pleistocene and episodically in the Holocene, the last time being in the 16th century AD, the Uzboy River reached the CS c. 300 km north of the site and 100 km south of the KBG in the Krasnovodsk Bay (Fig. 1B) (Syrnyov, 1962; Létolle, 2000; Leroy et al., 2007). Human diversions are likely over the last millennia in addition to those caused by slight seismic movements. The Uzboy brought a considerable supply of freshwater to the south basin. This river received water from the Sarykamysh Lake and the Amu-Daria directly from the Tien-Shan and Pamir, hence from a drainage basin under a climate totally different from that of the Volga River basin that is under the Westerlies (Ferronsky et al., 1999; Chen et al., 2008; Fig. 1A).

The CS water is brackish with a gradient from the north to the south from freshwater where the Volga enters the sea, to 13 psu in the east and south-east corner (Rekacewicz, 2007a). The mean sea surface temperature in winter ranges from zero in the north to 10 °C in the south, and in summer from 21 in the east to 28 °C in the south (Rekacewicz, 2007b).

The CSL fluctuates close to 27 m below sea level. It is very sensitive to changes in the precipitation over the Volga basin and to changes in evaporation over the basin itself (Arpe et al., 2012; Fig. 1A).

The climate in the Gomishan area has a typical semi-arid climate: dry and hot in the summer and cool in winter, a mean annual precipitation of 300 mm and a mean annual temperature of 17.5 °C (Honardoust et al., 2011). The natural vegetation is *Halocnemum strobilaceum*, *Aeluropus littoralis* and *Puccinellia distans* (Poaceae), *Tamarix ramosissimum* and *Suaeda maritima* and *Salsola rigida* (Chenopodiaceae). The staple crops are winter barley and wheat (Honardoust et al., 2011).

The vegetation of the Gomishan lagoon itself is very diverse and dominated by halophytes. *H. strobilaceum* and *Salicornia europaea* (Amaranthaceae), *S. rigida* and *Halostachys caspica* (Chenopodiaceae), *T. ramosissimum and T. galica* are dominant in the E and NE because of the higher salinity environment. The lagoon also exhibits a range of aquatic plants such as *Potamogeton pectinatus, Zannichellia palustris, Ruppia maritima* and *Ceratophyllum demersum*, especially in the N and NW (Karimi, 2010).

The vegetation on the northern slope of the Alborz Mountains presents a series of east–west belts, from bottom to top, starting with a steppe with *Artemisia* and *Astragalus* at sea level, followed by the Hyrcanian forest up to c. 500 m interrupted in the drier areas by a forest of *Thuja orientalis* east of Gorgan, then by the oak, hornbeam and beech mountain forest up to c. 2000 m. A slightly drier *Quercus macranthera* forest developed up to c. 2500 m, then Juniper woodland and the alpine meadows (Akhani et al., 2010; Encyclopaedia Iranica, no date).

The Gorgan wall, which forms a prominent archaeological defensive feature in the region, is a brickwork associated with forts and waterworks, over 195 km long and extends west–east at the foot of the Alborz Mountains. It served the same purpose as the Great Wall of China but is shorter. The Sasanian Empire built this wall in the 5 or 6th century AD when the CSL was several metres lower than now. In the westernmost section it is now covered by marine sediment (Omrani Rekavandi et al., 2008) probably dating from the Little Ice Age (LIA) highstand. The area between the Gorgan Wall and the Alborz highland has been cultivated and was renowned for its fertility for a long time, as testified by the density of archaeological sites. A significant number of archaeological sites has nevertheless been mapped north of the wall as well, although this part of the region was mostly devoted to nomadic pastoralism (Nokandeh and Sauer, 2006).

3. Past investigations

3.1. Palynological analyses in the region

No complete Holocene diagram is available for the region. Each of the following six investigations covers part of the Holocene (Fig. 1B).

A deep marine sediment core (core **GS05**) provides vegetation history and sea level changes for the Lateglacial and beginning of the Holocene (Pierret et al., 2012; Leroy, unpublished). The pollen diagram shows the development of shrubs at the beginning of the Holocene followed by the development of trees delayed however by a few millennia. The geochemical analyses reveal mechanical erosion during glacial times followed by chemical weathering during the interglacial. The dinoflagellate cysts remain dominated by low salinity assemblages (c. 7 psu) until 3.9 cal. ka (Leroy et al., 2007; Leroy, unpublished data).

Leroy et al. (2007) published the results of a joint pollen and dinocyst study of marine cores, one of them from the south basin of the CS, close to core GS05, which covers the period ca 5.5–0.8 cal. ka BP (core **CP14**). Two phases of higher sea levels with a stronger river influence and low salinity were identified: one from the core base until 3.9 cal. ka BP and one from 2.1 to 1.7 cal. ka BP.

A pollen diagram from the **Muzidarbon** mire near Nowshahr at 550 m altitude (Ramezani et al., 2008) covers the last 1000 yr. It suggests a possible record of the Medieval Climatic Optimum and the LIA. A clear increase in human activity is seen since the beginning of the 19th century. The coastal lagoons of **Anzali** and **Amirkola** (Leroy et al., 2011) provided a record of the last four centuries indicating higher CSL during the late LIA. A palynological study of the last 200 yr was obtained from a core in the NW of the **Kara-Bogaz Gol**, where human activities on water level control were by far the strongest signal in the proxies (Leroy et al., 2006).

Modern pollen samples are available for the **Golestan National Park** across a transect from the Hyrcanian forest to an *Artemisia* steppe from 800 to 1800 m altitude (Djamali et al., 2008, 2009) and in the lagoons of Anzali and Amirkola (Kazancı et al., 2004; Leroy et al., 2011). They provide a useful link between pollen rain and vegetation. Various types of surface samples were compiled for **Turkmenistan**, including from the SW of the country, near the Iran-Turkmenistan border (Peterson, 1983).

3.2. Sedimentology, chronology and palaeoenvironmental reconstructions of the TM core

The details of the sedimentological and chronological study of core TM, taken in a palaeo-lagoon connected to the Hassan Gholi Bay, have been published by Kakroodi (2012) (Fig. 2). Eight lithozones were defined on the basis of the visual description of the sediment, which is generally fine-grained with some rare sandy silt layers, and macrofossil assemblages, i.e. shells, large diatoms, Charophytes and ichnofossils. Ten radiocarbon dates obtained on shells (ostracods, foraminifera or gastropods) show no reversals (Table 1), They were used for building the age–depth model after calibrating by Marine09 (Reimer et al., 2009; Kakroodi, 2012).

The deposits show three major regressive stages, one at the base, one in the middle and one at the top of the core (Kakroodi, 2012) (Fig. 2). Late Pleistocene deposits containing typical Pleistocene fauna and loess and dated around 17,367 ^{14}C BP or 20,160 cal. yr BP calibrated (Lithozone 1) are separated by a hiatus from the Holocene deposits suggesting a CSL fall. Large gypsum crystals, up to 4 cm length, are found at the top of this lithozone. Radiocarbon dated shell suggests that, after the deep Late Pleistocene/Early Holocene regression, the initial transgression (lithozone 2) started before 9717 ^{14}C BP or 10,640 cal. yr BP. Following postglacial sea-level rise, modern fauna started to develop from then on. This CSL rise was characterised by the deposition of coarse silt and abundant fauna in a lagoonal environment. Continuous sea level rise led to landward shift of the lagoonal system, and hence increasing accommodation space and changes in biofacies depth (lithozone 3). Diatom and Gastropoda species developed in this deeper environment within silty and clayey deposits up to around 7120 ^{14}C BP or 7595 cal. yr BP (lithozone 4). After this highstand, sea level started to fall again, and reddish oxidised sediments with abundant foraminifera (*Ammonia beccarii*) recorded a regressive facies (lithozone 5). A probable minor hiatus at 12.10 m depth is suggested by the mottling of the sediment and thin layers of evaporites (gypsum crystals up to 2 cm length). Lithozone 6 is characterised by dark silty clays representing lagoonal facies, followed by the olive clayey silts indicating shallow marine to hypersaline conditions (lithozone 6). Lithozone 7 is interpreted as a shallow lagoonal environment strongly influenced by terrigenous input. In lithozone 8, the highest values of sand and the presence of frequent ichnofossils of insects, probably Trichoptera, occur. The sediment is mostly an alternation of brownish lagoonal clays and barrier sands, in a highly oxidising environment. The difference between lithozone 8a and 8b is based on the increase of rootlets, ichnofossils and traces of oxidation.

4. Material and methods

4.1. Samples

This investigation bears on the palynological analysis of core TM and is supported by surface samples. The surface samples come from coring, grabbing, and/or the scooping of marine, lagoonal and river muds as well as mosses.

The 27.7 m long core, called TM, was taken in 2009 by percussion and a rotary hydraulic drilling rig, located at 37° 09′ 06″ N, 54° 03′ 24″ E and 2 m above present sea level (i.e. ~25.5 m bmsl). The

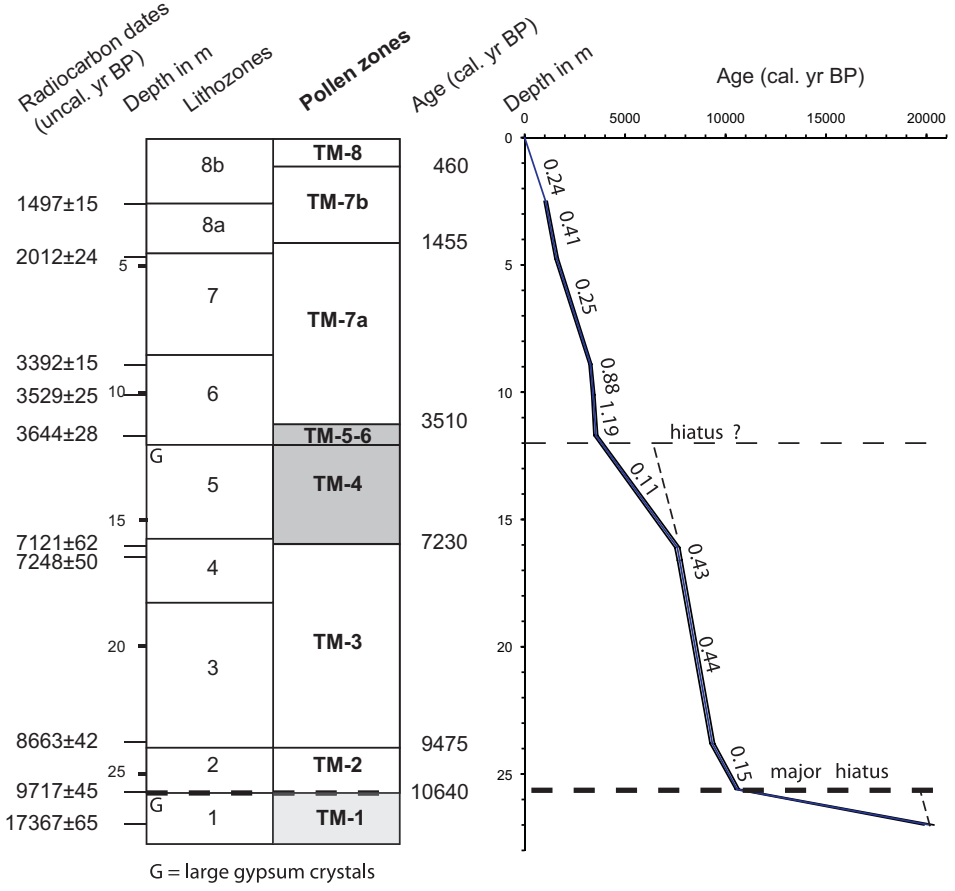

Fig. 2. Lithology and age–depth model for the TM sequence, Gomishan. The confidence interval for the calibrated radiocarbon is plotted with 2σ. The two grey rectangles in the pollen zone column indicate sterile zones. Sedimentation rates in mm per year.

Table 1
Radiocarbon dates of the TM sequence calibrated by calib6.0 with MARINE09.14c (Reimer et al., 2009).

Composite depth in cm	Sample name	Material	Laboratory number	Uncalibrated age	Reported error	Calibrated age[a] in BP, 2 sigma	
2.5	no6top	Gastropoda	NZA34283	1497	15	1120	969
4.75	gm2n10d91	Broken bivalves	UBA-20606	2012	24	1672	1507
8.9	no18La	Gastropoda: Theodoxus	NZA34285	3392	15	3337	3203
10.1	no20 17cmB	Ostracoda: Cyprideis	NZA34120	3529	25	3488	3338
11.7	tm31	Gastropoda	UBA19908	3644	28	3633	3449
16.1	gm2n31d41	Many ostracoda & foraminifera	UBA-20607	7121	62	7718	7474
16.6	no3110cm top	Foraminifera: Ammonia beccarii	NZA34427	7248	50	7827	7603
23.8	gm2n43d9	One bivalve	UBA-20605	8663	42	9450	9228
25.6	no45 5 cm B	Gastropoda: Ps. brusiniana	NZA34121	9717	45	10,681	10,492
27	no47B	Ostracoda: Cyprideis	NZA34122	17,367	65	20,370	19,876

[a] Calib6.0 MARINE09.14c.

diameter of the core is 5.5 cm and the length of each drive was 60 cm. A casing was used to prevent hole collapse.

Table 2 provides a brief description of the sampling locations of the modern samples. For the marine and lagoon samples, information on water salinity has been added where available.

4.2. Treatment, identification and statistical analyses

Initial processing of the 48 core (1.5–2.5 ml in volume) and 43 modern samples involved the addition of cold sodium pyrophosphate to deflocculate the sediment. Samples were then treated with cold hydrochloric acid (10%) and cold hydrofluoric acid (32%), followed by a repeat HCl. The residual fraction was then screened through 120 and 10 μm mesh sieves and mounted on slides in glycerol. The number of pollen and spores counted was usually around 350. *Lycopodium* tablets were added at the beginning of the process for concentration estimates (in number of specimens per ml of wet sediment) in the core samples only. In addition the moss samples were acetolysed.

Pollen percentages were calculated on the terrestrial sum (excluding aquatic, spores, unknown or unidentifiable pollen, and non-pollen palynomorphs). The diagrams were plotted with psimpoll4 (Bennett, 2007). A zonation by cluster analysis (CONISS) after square root transformation was applied. The zonation, based only on terrestrial taxa, was calculated for the percentage diagrams.

The dinocysts were counted at the same time as pollen and other microfossils. Identifications of the dinocysts are based on Marret et al. (2004), Mertens et al. (2009), Leroy (2010) and Mudie et al. (2011). The cysts of *Lingulodinium machaerophorum* have processes of various shapes and lengths, which have been counted separately (following form names defined in Leroy et al., 2006). Later on it has been suggested that the length may be linked to water summer salinity and to some extend to water temperature (Mertens et al., 2009). The total sum for dinocyst percentage calculations is made for all dinocysts, except *Brigantedinium* spp that is calculated on the sum of the dinocyst excluding *Brigantedinium* spp. The foraminiferal linings were calculated in the same way as the latter.

A ratio, pollen concentration on dinocyst concentration (P:D), was calculated according to McCarthy and Mudie (1998) to establish the terrestrial influence versus the marine one, the higher the ratio the stronger the terrestrial influence.

5. Results and interpretation

5.1. Modern samples

The samples were first grouped by type of archive, from top to bottom: marine sediment, lagoonal sediment, muds (mostly rivers and lakes), and finally mosses (Fig. 3). Then within these four groups the samples are arranged geographically from the north to the south, and then from the east to the west with the south-east corner of the region taken as a pivot point. This is approximately where the long core is located.

When combining different types of surface samples, a primordial role is played by the type of archives in differentiating the assemblages, and the potential influence of the archive type needs to be examined before searching for geographical differences (Leroy et al., 2009). In general the muds and the mosses have higher Arboreal Pollen (AP) percentages. This is due to their location that is often closer to forests. The exceptions to this are the saiga dropping and a black ground moss on the shores of the Aral Sea. In contrast to the moss samples, the marine and lagoonal sediment have more Amaranthaceae–Chenopodiaceae (A–C) and *Artemisia* due to the proportional increase of long-distance transport. The lagoonal samples have the richest diversity of aquatic plants although *Typha-Sparganium* is found nearly everywhere due to its good dispersal in open environments, especially steppes (Bottema and Barkoudah, 1979). Spores are mostly present in the marine sediment and in the Gorgan delta and the Babolsar river mouth. The least well-preserved palynomorphs are found both in the marine sediment and in the mosses. The NPPs, Incertae Sedis 5b and 5d, *Pterosperma* and *Radiosperma* are found more often in the marine sediment, whereas the algae (*Botryococcus* and the Zygnemataceae) and Cyanobacteria (*Anabaena* and *Gloeotrichia*) are indicators of lagoonal settings.

5.1.1. The dinocysts and the foraminiferal lining

The marine samples and the lagoonal samples had sufficient numbers of dinocysts to build a separate percentage diagram of dinocysts (Fig. 3). This illustrates a contrast between the marine samples (except US24 and 26) that have more *Impagidinium caspienense* and *L. machaerophorum*, whereas the lagoonal samples have slightly higher levels of dinocyst taxa tolerating fresher conditions such as *Spiniferites cruciformis*. Besides this, the two samples from the northern part of the middle basin, US24 and US26, show considerable amounts of *Pentapharsodinium dalei, S. cruciformis* and *Caspidinium rugosum rugosum*, taken as reflecting the lower salinities of this part of the CS. Some marine and the lagoonal muds also contain the lining of benthic foraminifera that live in the CS in waters no deeper than 50 m (Kh. Saidova, pers. comm.; Boomer et al., 2005). The P/D ratio is clearly higher in the lagoonal surroundings than in the marine samples, clearly illustrating the close proximity of the land.

5.1.2. Geographical gradients

The marine samples (except the northern most ones US24 and 26) show an increase of the *Alnus* percentages westwards reflecting

Table 2
List of surface samples from the south-east and east of the Caspian Sea area.

Sample label	Latitude N	Longitude E	Altitude in m/water depth in m	Brief description of location	Sampling date	Type of sample	Surface salinity	Salinity source
US24	43 19 14	49 06 02	61	Core top	Aug. 1994	Marine	9.5 (snapshot)	F. Chalié
US26	43 19 36	49 05 58	61	Core top	Aug. 1994	Marine	9.5 (snapshot)	F. Chalié
Torkmen 20 m	37 05	53 35	−27/20	Grab for phytoplankton	Winter 2010	Marine	9–10 (annual)	H. Nasrollazadeh
CS10	36 48 25.0	52 33 02.8	−27/250	Core top, core CS10 at 2 cm depth	2007	Marine	12 (snapshot)	Not measured at sampling; Jamshidi and Bin Abu Bakar, 2011 for a station with 42 m water depth in 2008
Babolsar 100 m	36 49	52 39	−27/100	Grab for phytoplankton	Jan-11	Marine	9.5–13 (annual)	H. Nasrollazadeh
Babolsar 20 m	36 46	52 40	−27/20	Grab for phytoplankton	Jan-11	Marine	8–11.4 (annual)	H. Nasrollazadeh
Almagol	37 25 53.50	54 38 52.18	0/0.6	Core top in Modern Lagoon	Sep-10	Lagoon	2–3 (annual)	Not measured at sampling; Patimar 2008
Alagol	37 21 59.48	54 34 44.33	−6/0.6	Core top in Modern Lagoon, water at −6 m	Sep-10	Lagoon	3.5–4.0 (annual)	Not measured at sampling; Patimar 2008
TR1	37 03 43.70	54 01 59.02	−27/0.1	Core top in Modern Lagoon (Gm1 short)	Sep-10	Lagoon	20–24 (Spring–Summer)	Not measured at sampling; Patimar et al., 2009 for 2007
BTorkman2	36 53 57.3	54 02 46.1	−27/c. 0.1	Scooping of mud in artificial pool behind bay, reeds, Salicornia	20-May-11	Lagoon	22 (spring)	S. Leroy
BTorkman1	36 53 49.7	54 02 39.4	−27/c. 0.1	Scooping of mud in Salicornia meadow in habour	20-May-11	Lagoon	17 (spring)	S. Leroy

Sample label	Latitude N	Longitude E	Altitude in m	Brief description of location	Sampling date	Type of sample
Ashyagar	43 35 38.7	51 39 50.2	−125	River mud in Karaghiye depression	21-May-06	Mud
Karakol	43 24 22.2	51 20 28.1	−27	Core top, 0–1 cm	21-May-06	Mud
SD10PVC4	43 35 09.4	58 32 29.2	53	Core top, phragmitaie	20-Sep-10	Mud
Amu-Daria canal	43 10 28	58 34 48	53	Along canal edge	13-Sep-10	Mud
S. Aral phragmites	43 08 55	58 38 04	56	Phragmites in steppe	13-Sep-10	Mud
Chilpak-Kala 1	42 15 54.4	60 04 55.8	80	In phragmites near achaeological site	12-Sep-10	Mud
Chilpak-Kala 2	42 15 54.4	60 04 55.8	80	In open pond near achaeological site	12-Sep-10	Mud
Amu-Daria bridge	42 13 26.2	60 06 26.6	91	Mud along river near Tortkul village, maize & cotton fields and Populus along shores	12-Sep-10	Mud
Amu-Daria Tortkul	42 13 20	60 06 55.5	70	Mud along river near Tortkul village, maize & cotton fields and Populus along shores	12-Sep-10	Mud
S. Aral Bogolon	41 42 40	60 31 08	95	Dirty puddle between Gurlan and Urgench, very near Bogolon, a lot of cow pads & straw	12-Sep-10	Mud
Bahardok	38 48 27.8	58 29 0.35	70	Shore of small lake in a depression in the Karakum near the village of Bokdyrak (PPKI, Bahardok), Turkmenistan	Mar-12	Mud
TR2	37 09 04.22	54 00 11.10	−28	Core top in Modern Lagoon (Gm2 short)	Sep-10	Mud
AqQaleh	37 00 52.06	54 27 38.06	−12	Core top in river, near bridge	Sep-10	Mud
Gorgan delta	36 58 39	54 01 00	−27	Delta between zones of phragmites and chenopods, Iranian Artemisia steppe	8-May-05	Mud
BTorkman3	36 54 03.9	54 03 17.1	−27	Puddle along road, between road and railway, salinity 11, Salicornia, submerged plants, eutrophic, green water	20-May-11	Mud
KaraSu 3	36 49 40.9	54 02 14.0	−27	River mouth, high energy, salinity 13, old clays being eroded by waves	20-May-11	Mud
KaraSu 4	36 49 39.8	54 02 31.3	−27	Riverside mud, salinity 10, submerged plants, reeds	20-May-11	Mud
KaraSu 5	36 49 39.8	54 02 31.3	−27	Further inland, perhaps old mud, salinity 6	20-May-11	Mud
KaraSu 1	36 49 33.4	54 02 32.6	−27	Artificial lagoon inside natural lagoon, no submerged plants, Tamarix, salinity 98	20-May-11	Mud
KaraSu 6	36 49 32.4	54 02 55	−27	*Lemna, village bridge, salinity 1*	20-May-11	Mud
KaraSu 2	36 49 29.0	54 02 33.1	−27	Natural lagoon, Tamarix, reeds, submerged plants, salinity 24	20-May-11	Mud
Nahar Khoran 2	36 46 01	54 28 11.2	18	River mud	19-May-11	Mud
Nowkandeh river	36 44 53.4	53 54 19.4	c. −27	Small river, out of city, in the fields, from riversides, very polluted, cattle drinking & sewage, eutrophic water	19-May-11	Mud
Babolsar River	36 42 23.6	52 38 57.9	c. −27	In the city, near harbour, along river sides	19-May-11	Mud
Aral black moss	45 06 04.5	58 19 28.5	51	On ground near Haploxylon & Tamarix	14-Sep-10	Moss
Saiga	45 06 02.1	58 19 58.3	48	Whole half of dropping, Saiga dropping, Aktumsiq lowland	15-Sep-10	Moss
Nahar Khoran 1	36 46 01	54 28 11.2	18	On bark in Gorgan jungle	19-May-11	Moss
Huto cave	36 41 25.57	53 29 48.86	24	Cave entrance, Behsahr, Tarujen	7-May-05	Moss
Gomishan	36 40 14	53 21 57	33	Cave entrance, Neka-Beshahr	7-May-05	Moss
Firuz Kuh 230	36 15 17.5	52 54 01.5	230	On soil along road, forst on slopes, fields on valley bottom	20-May-11	Moss
Firuz Kuh 700	36 04 00.9	53 04 23.7	700	On bark, damaged woodland, agriculture, conifer plantations	20-May-11	Moss
Firuz Kuh 1550	35 53 52.6	52 58 59.9	1550	Low moss on shaded soil below trees at base of cliff, rather dry	20-May-11	Moss

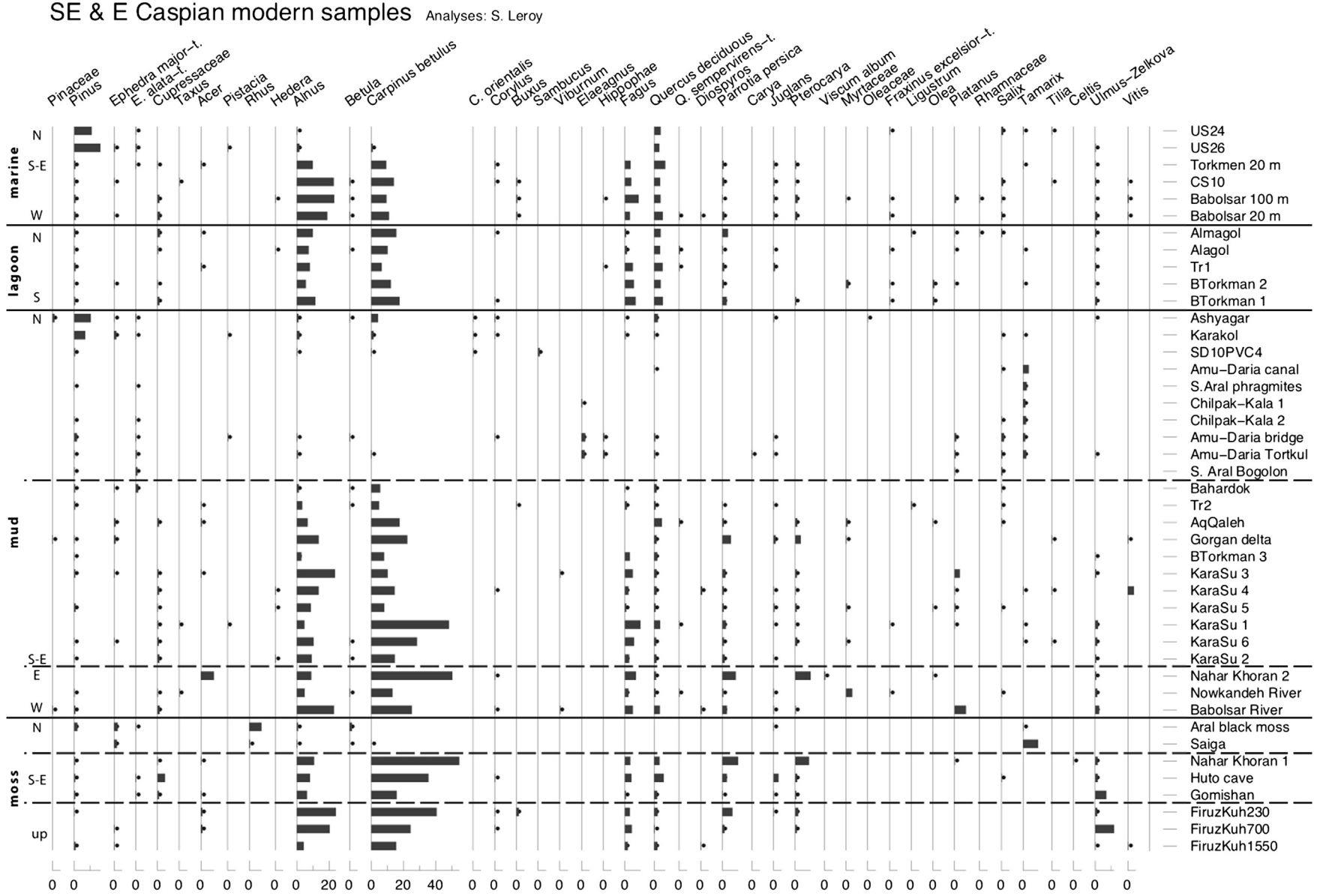

Fig. 3. Palynological diagram for surface samples of the south-east and east of the Caspian Sea area. Concentration in number of palynomorphs per ml of wet sediment. Black rectangle on Fig. 3d shows the dinocyst diagram.

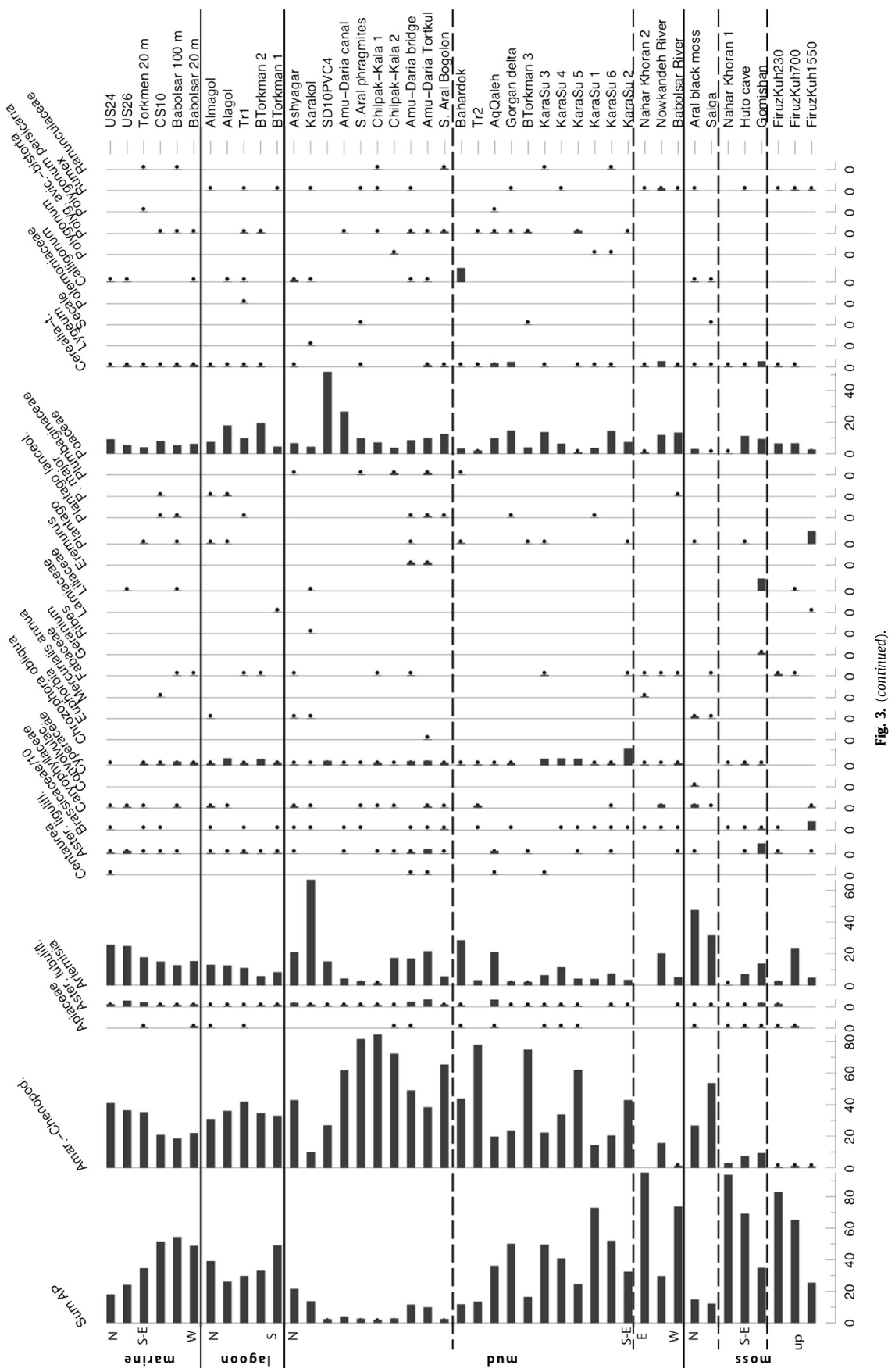

Fig. 3. (*continued*).

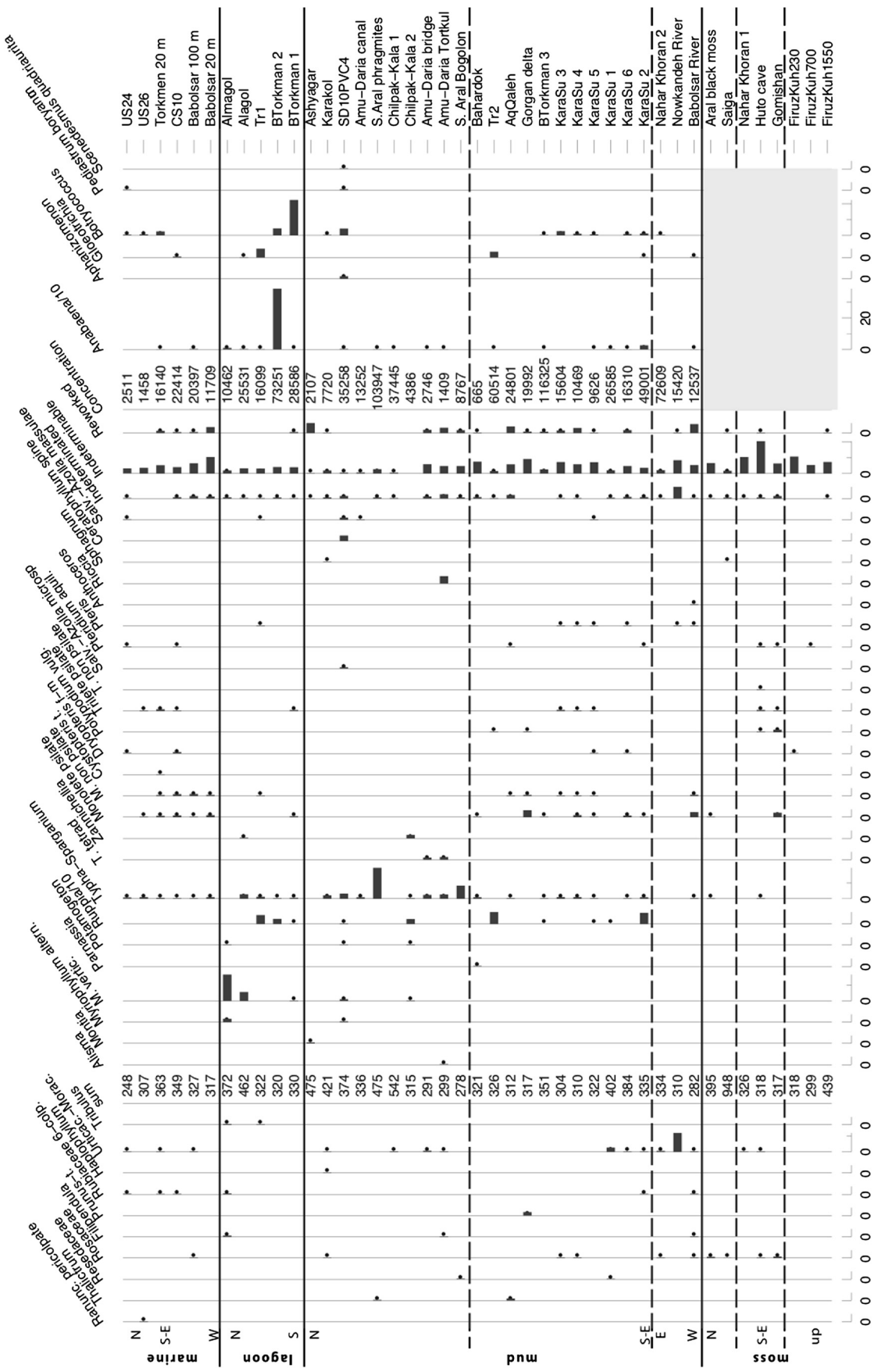

Fig. 3. (*continued*).

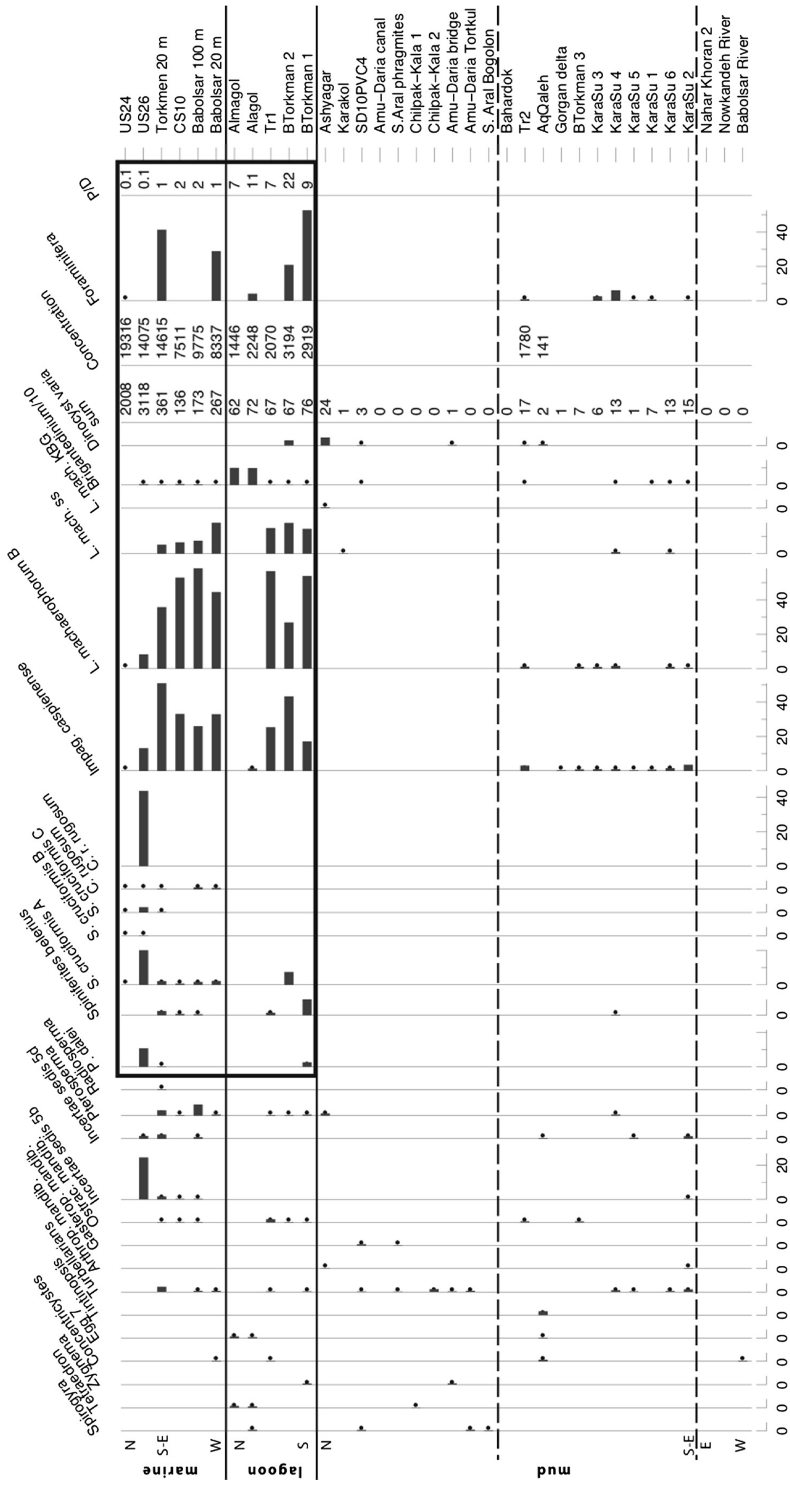

Fig. 3. (continued).

well the increased development of the coastal alder forest following the increased precipitation gradient westwards (location in Fig. 1C). The five lagoonal samples (in Golestan) still contain close to 10% of alder pollen although *Alnus subcordata* does not grow in Gomishan lagoon (Tr1), Almagol and Alagol, owing to its sensitivity to salt (Browicz, 1982; Honardoust et al., 2011; Naqinezhad, pers. comm.). The distribution of *A. subcordata* trees seems to be limited to south of the Gorgan River. It is clear that this frequently over-represented pollen is wind transported north of the Gorgan River. Peterson (1983) also noted relatively high percentages of alder pollen in South West Turkmenistan.

The northern subgroup of the mud sample group (Kazakhstan and Uzbekistan) has very little arboreal pollen. The significant percentages or *Pinus* in the two Kazak samples, Ashyagar and Karakol, are noteworthy, probably linked to the proximity of villages with ornamental/commercial trees. The highest numbers of A–C are reached with occasionally high Poaceae when the samples are taken from a *Phragmites* marsh: e.g. Sudochie (SD10PVC4), just south of the Aral Sea. The southern subgroup (Iranian Turkmenistan) has surprisingly high percentages of AP (*Carpinus betulus, Fagus orientalis, Quercus, Parrotia persica* and *Pterocarya fraxinifolia*) despite the openness of the landscape; this is explained by the strong influence of the pollen rain from the forested slopes of the Alborz. Anomalously high percentages of *Carpinus* (5%) were noted in the surface samples of SW Turkmenistan (Peterson, 1983). The alder pollen, as in the lagoons of the west coast of Golestan, is wind transported from the southern coast of the CS. The three samples from the south were taken in the forest (Nahar Khoran) or in more intensely transformed landscapes (Nowkandeh and Babolsar). The latter is reflected by high AP values and the high values of planted trees (*Platanus* and Myrtaceae such *Eucalyptus*) as well as the NAP such as *Cerealia*-t., Urticaceae-Moraceae and *Rumex*.

Near the Aral Sea, the saiga dropping and the black ground moss have extremely low AP percentages, mostly pollen derived from bushes of dry environments, such as *Rhus* and *Tamarix*. They have one of the highest *Artemisia* values, which are clearly originating from the steppe environment. This is in common with the muds from the same region and close to the percentages of the marine samples, although in the latter case the pollen of *Artemisia* is obviously wind transported over long distances. According to Peterson (1983) high percentages of *Artemisia*, >40%, are only reached in the mountains of Tadzhikistan and Kirghizstan (see also Giralt et al., 2004). The three southern moss samples are derived from an increasingly degraded environment westwards, which is seen in the drop of AP, especially of *C. betulus*. The short altitudinal transect to the Firuz Kuh (pass in the Alborz at 2220 m altitude) from 230 m to 1550 m altitude shows the same decreasing trend in AP.

5.2. Core TM

The results and interpretation are presented based on the terrestrial pollen zonation (Fig. 4).

5.2.1. Pz TM-1, 27.7–25.7 m (lithozone 1), Late Pleistocene and onset of the Holocene

Three samples indicate that this zone is sterile in palynomorphs. The lithological reconstruction proposes a marine unit mixed with reworked loess that has been profoundly oxidised during a subsequent regression. This lithozone ends in a sharp erosional horizon.

5.2.2. Pz TM-2, 25.7–24.0 m (lithozone 2), 10,640–9475 cal. yr BP

A–C largely dominates the terrestrial pollen spectra of the four samples; the other herbaceous taxa are *Artemisia* and Poaceae. Some tree pollen are present such as deciduous *Quercus*, and very low amounts of *C. betulus* and *Alnus*.

The Chenopod pollen, belonging to an anemophilous family with strong pollen productivity, is primarily derived from the semi-desert in the region, and only secondarily from local saltmarshes (Horowitz, 1992). The extremely high percentages reached here (>60%) are seen in the surface samples only in the saltmarshes of the Iranian Turkmenistan (Karasu and Gomishan) or in the semi-desert south of the Aral Sea (eg Chilpak-Kala, Amu-Daria canal and S. Aral Bogolon). Peterson (1983) has noted up to 40% of Chenopodiaceae in western Turkmenistan.

The landscape is a semi-desert locally, probably with salt marshes, with a minor influence of forested areas with oaks in the nearby mountains.

The dominance of *I. caspienense*, a dinocyst characteristic of brackish waters such as the modern day water (salinity 13 psu; Leroy et al., 2007), Incertae Sedis 5b (present in the marine samples of the modern dataset and in the marine cores CP14, CP18 and CP21, Leroy et al., 2007) and the organic lining of foraminifera indicate a marine influence; however a coast with a lagoon cannot be far as pollen grains of *R. maritima* are observed.

Lithology suggests a lagoonal deposit in broad agreement with the palynological interpretation, as the latter proposes open water influence.

5.2.3. Pz TM-3, 24.0–15.7 m (lithozones 3 and 4), 9475–7500 cal. yr BP

In the first part of this unit *Artemisia,* Asteraceae Liguliflorae and *C. betulus* percentages increase sharply; whilst in the second part, a peak of arboreal pollen is marked with maxima of deciduous *Quercus, C. betulus* and *P. persica*, reflecting a vegetation optimum and the extension of forest belts towards the steppic plain (but far from reaching it). Surface samples such as at AqQaleh, the Gorgan delta and in the western part of the Karasu show similar values of *C. betulus* pollen in the absence of forest.

This is the most marine/open water unit of the whole diagram, with minimal continental influence. The pollen concentration in this zone is at first high, but then declines.

Lithological reconstructions indicate a low energy environment with a shallowing at the top of lithozone 4.

5.2.4. Pz TM-4-5-6, 15.7–11.3 m (lithozones 5 and 6 pp), 7500–3510 cal. yr BP

Seven out of eight samples are devoid of palynomorphs making the sediment of Pz 4 to 6 quasi sterile. The lithology reflects periods of shallow water and/or emersion, and is therefore a generally not favourable sediment to palynomorph preservation.

5.2.5. Pz TM-7, 11.3–1.1 m, 3510–460 cal. yr BP (lithozones 6 pp to 8 pp)

Although not suggested by CONISS, a practical and logical subdivision of the nineteen samples in two subzones could be made at c. 4.2 m depth.

5.2.6. Pz TM-7a (lithozones 6 pp, 7 and the beginning of 8a), 3510–1455 cal. yr BP

The terrestrial environment is now clearly a steppe with percentages of *Artemisia* similar to those along the coast of Kazakhstan (Karakol and Ashyagar). The coastal strip is covered by an alder carr that is a wetland with an alder forest (Leroy et al., 2011). The distant influence of the deciduous forest is marked by *F. orientalis* and *P. fraxinifolia* pollen. Pollen of *Cerealia*-t. is frequent. In the Middle East, it is usually impossible to separate domesticated cereals from wild ones; both are probably present in the region at the time. Therefore *Cerealia*-t. pollen on its own is not sufficient to confirm

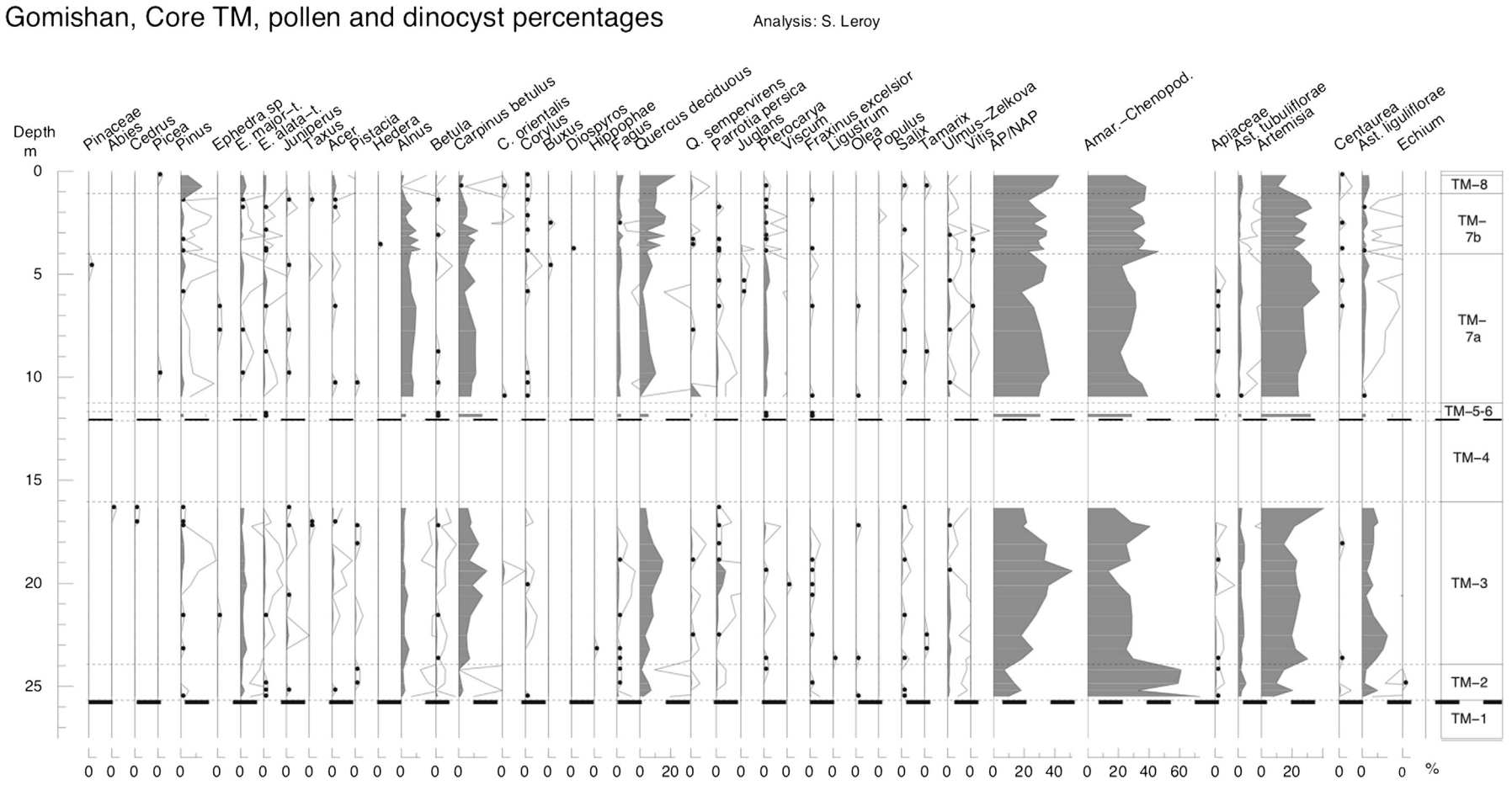

Fig. 4. Palynological diagram for core TM, Gomishan. Concentration in number of palynomorphs per ml of wet sediment.

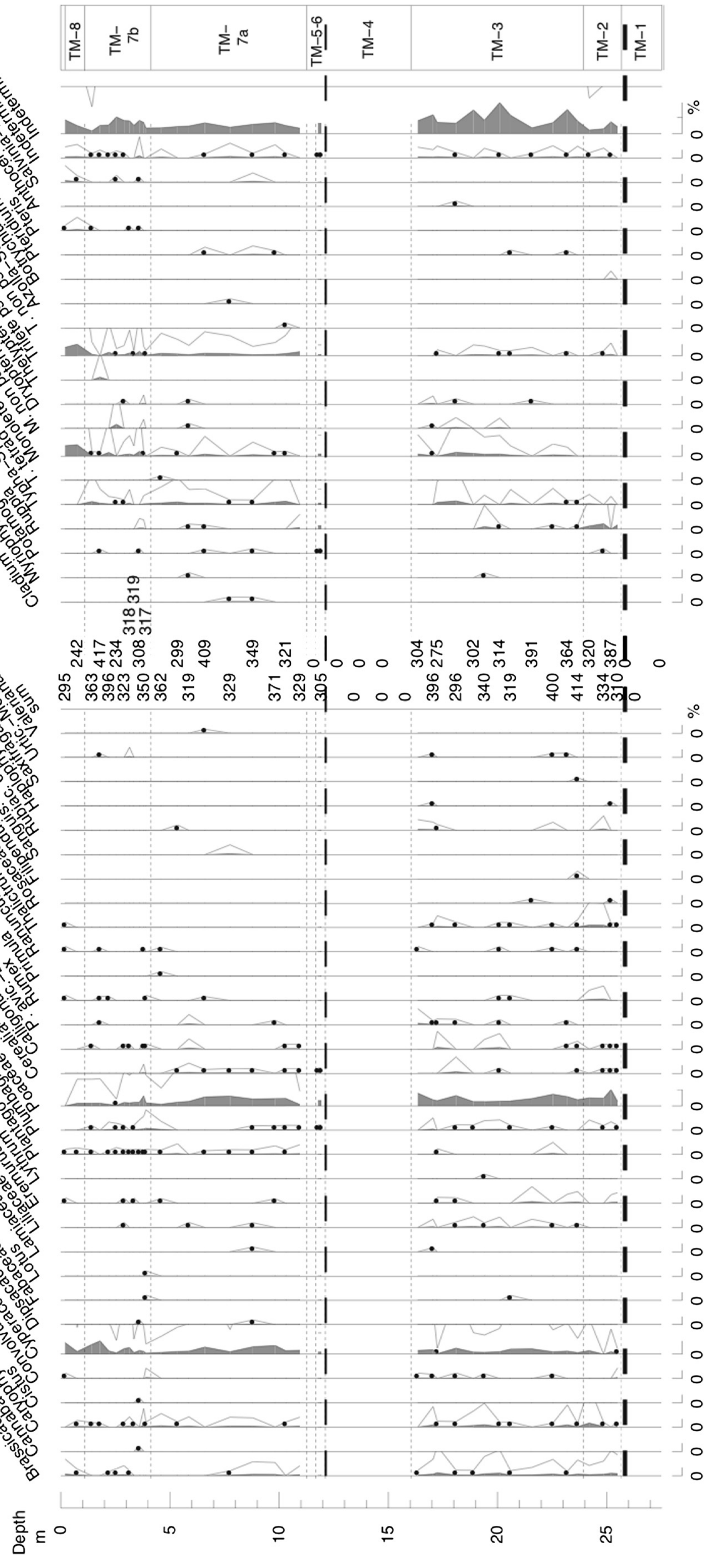

Fig. 4. (*continued*).

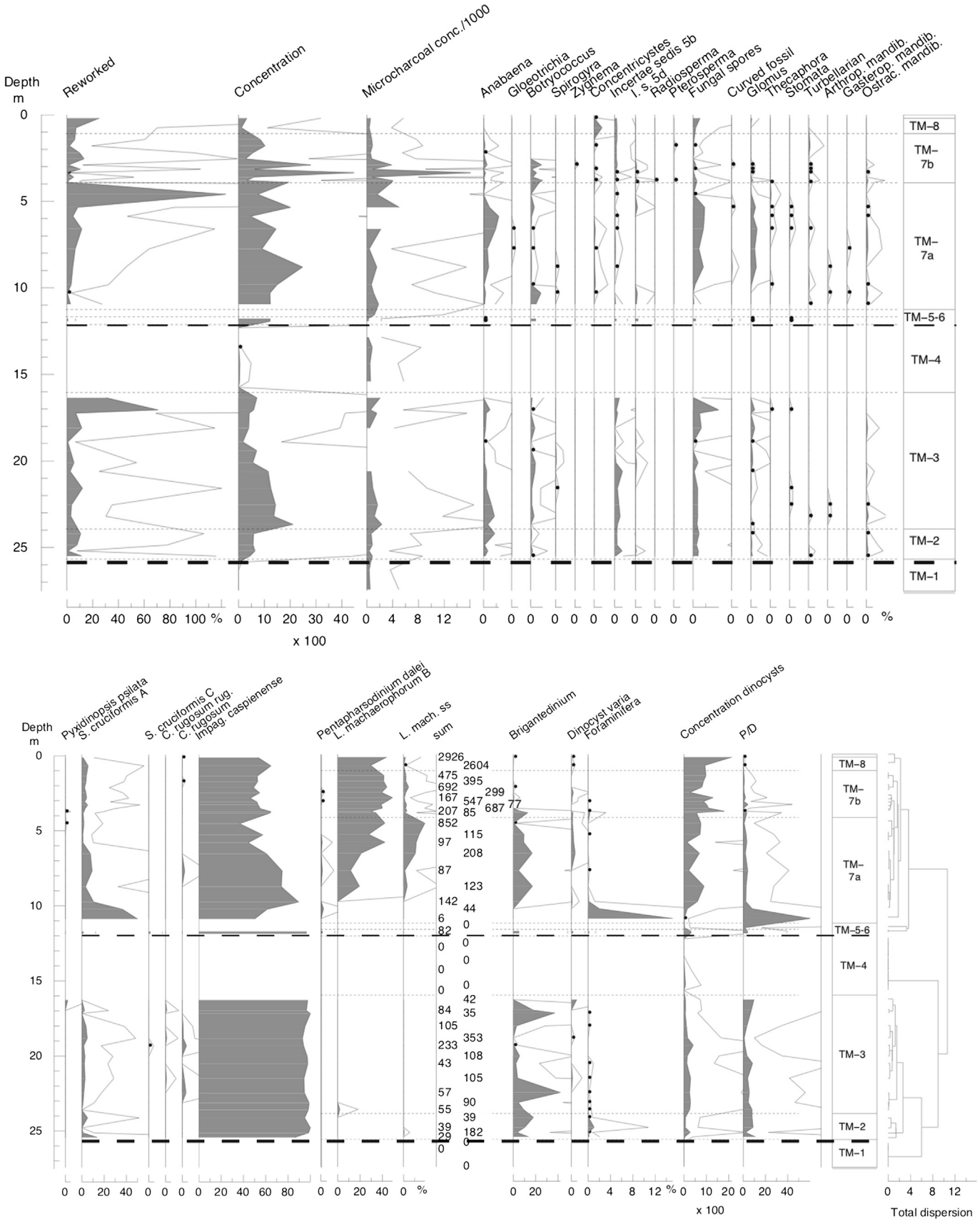

Fig. 4. (*continued*).

human activities (van Zeist et al., 2009). However here Cerealia-t. is found together with a continuous curve of *Plantago* and the occurrence of *Juglans* in the middle of the zone (only occurrence for the whole diagram). This allows suggesting that the landscape is already profoundly modified by humans. The amount of microcharcoals is progressively increasing through zone TM-7a.

In the first samples, the dinocyst assemblage contains very high percentages of the low salinity dinocyst, *S. cruciformis* (salinity c. 7 psu; Marret et al., 2004; Leroy et al., 2007), similar to the present-day lagoon of Anzali, further west along the Iranian coast (Kazancı et al., 2004). Foraminiferal linings display a strong peak. These two taxa sharply decrease in the middle of this subzone. The percentages of *I. caspienense* at first low during the peak of *S. cruciformis*, then rapidly reaching high values, finally progressively dropping to a minimum at the end of this subzone, due to the increase of two forms of *L. machaerophorum*. This succession indicates an increase in salinity (change in the process length) and temperature (increase biomass). *L. machaerophorum* ss, which peaks at the end of pz TM-7a before collapsing, has been linked to higher salinities than *L. machaerophorum B* (Mertens et al., 2009). Its collapse indicates a sharp drop in salinity, while temperatures probably remain the same.

Fungal spores are abundant, especially *Glomus*. The NPP, *Concentricystes*, is occasionally present. These latter taxa indicate a strong erosion of the nearby land in line with the high Ti/Ca values originating from terrigenous inputs (Kakroodi, 2012). This pollen zone starts with a slow increase of the palynomorph concentration until a peak is reached. This pollen subzone therefore presents the signs of rapid changes in the environment from freshwater influence to more saline waters and strong erosion: i.e. a lagoon that fills in.

Lithozone 7 is interpreted as a shallow lagoonal environment. This interpretation fits well with the palynological results.

5.2.7. Pz TM-7b (lithozones 8a pp and 8b pp), 1455–460 cal. yr BP

Poaceae fall to minimal values, while Cerealia-t. becomes inconspicuous. The steppe is now invaded by Amaranthaceae-Chenopodiaceae, whereas *C. betulus* and *P. fraxinifolia* values decrease; these can be taken as signs of aridification or intensification of pressure by humans on the environment, such as grazing. If the latter is correct, then the increase of microcharcoals in the previous zone that actually culminates here in TM-7b can be taken as an indicator of deforestation.

The values of *I. caspienense* are higher than at the end of the previous zone and are homogenously moderate across this unit, while the values of the form ss of *L. machaerophorum* collapse and those of form B maintain maximal values.

Fungal spores and *Glomus* values drop in this subzone.

The pollen concentration fluctuates widely and then drops. At the opposite, the dinocyst concentration curve shows consistent higher values than previously.

The sedimentary record and the biofacies indicate lagoon-barrier or spit environment. The palynological interpretation is slightly divergent here and would tend to suggest permanent submersion, despite rapid changes in the environment.

5.2.8. Pz TM-8, 1.1 m to core top (lithozone 8b pp), 460 cal. yr BP-core top

The clearly increasing percentages of *Quercus, Pinus* and *Acer* in the two samples of this zone result from the impact of afforestation (Sagheb-Talebi, 2004; Akhani et al., 2010). The recent Pine afforestation is mainly due to *Pinus sylvestris, P. brutia* and *P. eldarica*. Whereas *Pinus* pollen grains are found scattered throughout the diagram, it is only here that continuous percentages occur. The earlier pollen grains may have come from great distances. The nearest natural population of *Pinus* is now in the dry middle mountain slopes of Georgia and Azerbaijan, with *P. eldarica,* a species sometimes treated as a subspecies of *P. brutia* (Weinstein, 1989). This residual population may have been larger in the past. Cyperaceae and Asteraceae also develop slightly in this zone, indicating more dry open land. Moreover, the development of a salt marsh probably occurs where previously an alder carr existed.

The dinocyst and fungal spores values are similar to those of the end of the previous zone. *Concentricystes* and Pteridophyte spores reach a maximum in the top 75 cm. This is interpreted as an increasing fluvial influence, perhaps an old course of the Gorgan River, now further south.

The interpretation of lithozone 8b is a shallower lagoon than in lithozone 8a.

This assemblage at the top of core TM does not however correspond to the modern assemblages in three samples which are geographically close to the location of TM core: two core tops, TR1 and TR2, taken in the modern lagoon west of core TM location and a sample taken in the westernmost part of the emerged delta of the Gorgan River. This dissimilarity is due to the lateral difference in the sedimentation environment. The modern salt marsh is strongly represented by higher values of A–C than in the long core. *R. maritima*, a submerged plant of brackish waters, has extremely high percentages; some foraminiferal linings have been encountered, whilst the dinocysts remain discrete and are alternatively dominated by *L. machaerophorum* or by *I. caspienense*. Hardly any Pteridophyte spores are observed. On the whole the modern lagoon samples reflect a brackish environment without river influence, with no direct equivalent in the long core. The Gorgan surface sample has higher AP and fern spores percentages than in the TM core top, reflecting transport by a river that flows along the foothills of the forested eastern Alborz Mountains.

6. Discussion

6.1. High sea levels in the Early Holocene

The highest sea levels of the Holocene are reached in lithozone 3/pz TM-3 (Fig. 5). This is in agreement with the two Russian stratigraphies, whether this highstand is part of the Neocaspian or not. If compared to the present reaction of the CSL to the climate on the Volga River catchment, such high levels should correspond to wet conditions in the catchment in north-eastern Europe, often alongside low evaporation over the sea itself (Arpe et al., 2012).

However, such clear relationship did not exist in the Early Holocene due to the existence of an inflow into the south CS basin from the Uzboy River, whose course starts in the Pamir Mountains and the Tien-Shan via the Amu-Daria (Fig. 1A). Indeed, palaeochannels of the Uzboy in Turkmenistan were active in the early Holocene (Syrnyov, 1962; Létolle, 2000). In the first part of the Holocene, the glaciers in the Himalayas were large and fed by strong monsoonal precipitations (Goodbred and Kuehl, 2000; Owen et al., 2005; Wünnemann et al., 2010). Therefore meltwaters from the high altitude glaciers would have contributed to maintain the high water levels in the CS during the period 10,060–7000 cal. ka BP, even though the meltwater from the Eurasian ice sheet had nearly petered out and the climate in the drainage basin of the Volga River was still relatively dry (Chen et al., 2008). Lake Sumxi records (Gasse and Wei, 1996) and others in the western Himalayas show that lake levels were affected from 10 to 7 cal. ka by high monsoonal precipitation whereas at present the Asian summer monsoon does not penetrate so far. The exact timing of this period fits well with the high sea level period in the CS. It is therefore suggested that the CS high stands in the first part of the Holocene are driven by precipitation fallen >2000 km away under

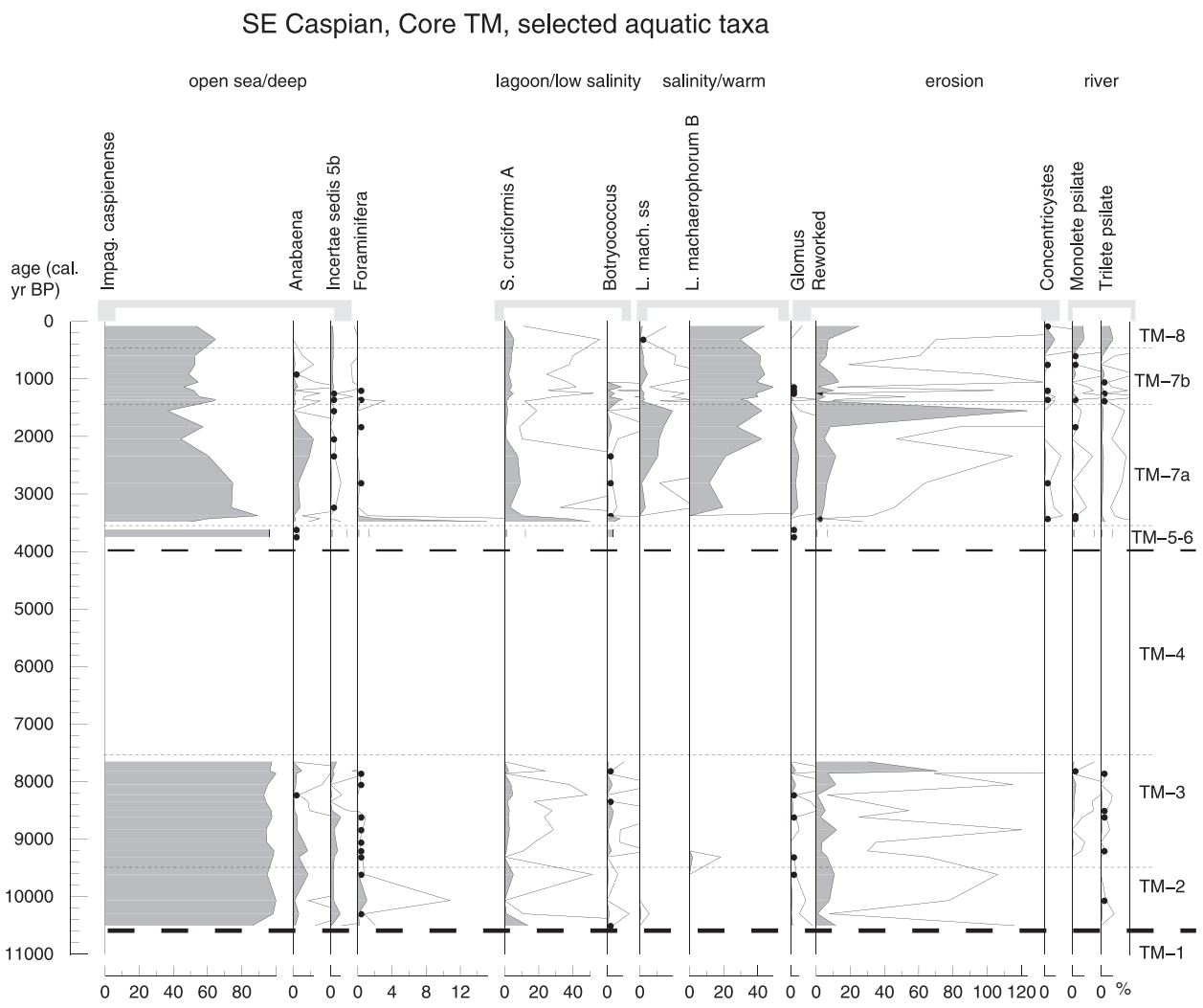

Fig. 5. Selected aquatic taxa from the diagram of core TM, Gomishan, plotted against time.

a completely different climatic regime, since, as soon as it leaves the Himalayas, the Amu-Daria (and then lower down the Uzboy River) crosses a dry region that does not contribute water to the river flow.

6.2. Lowstands at the Pleistocene/Holocene transition and in the mid-Holocene

According to Rychagov (1997) or Svitoch (2009), the beginning of the Neocaspian has a radically different age. Rychagov (1997) places the Mangyshlak at the transition Late Pleistocene/Holocene, whereas Svitoch (2009) places the Mangyshlak in the early–mid Holocene, retaining the name of Enotaev lowstand for the lowstand at the transition Late Pleistocene/Holocene. Both however agree on four lowstands: a Pleistocene/Holocene major lowstand, a minor lowstand at c. 8 ^{14}C ka, a major early–mid Holocene (7–6.5 ^{14}C ka) lowstand and finally a minor one at 4.5 ^{14}C ka BP. These two stratigraphies are mostly based on onshore studies. The rare exceptions are records from cores taken in the deep south and middle basins where the Neocaspian is assumed to have started at 10 ^{14}C ka BP, but where no signature of the Mangyshlak lowstand was found after the Khvalynian highstand probably due to the thickness of the water column which is able to buffer the impact of some sea level changes (Kuprin et al., 2003).

In the TM sequence, two major lowstands are clearly fitting the ages of the two main lowstands in the Russian literature (Fig. 5). Specifically, the Mangyshlak phase in Rychagov's terms corresponds to the low levels illustrated in the hiatus at 25.7 m depth at the very beginning of the Holocene. This is followed by another period, which may contain some hiati (Fig. 2), without palynomorphs somewhere between 7500 and 3510 cal. yr BP corresponding to the second main low stand of the Russian schemes in the early–mid Holocene, the Mangyshlak in Svitoch's terms. If there is a hiatus, it is most likely where the large gypsum crystals were found, i.e. near the top of this lithozone at 4000–3900 cal. yr BP.

A possible method for defining the Neocaspian is to use environmental conditions: here they indicate an intermediate CSL between the high stand of the Khvalynian and the low stand of the Mangyshlak; the conditions are also close to the present ones. Here the definition is based on the change in the salinity and temperature conditions of the CS waters characterised by dinocyst assemblages. In cores taken in the deep south and middle basins, parallel to those of Kuprin et al. (2003), a succession from *S. cruciformis* and *P. psilata*-dominated assemblages to an *I. caspienense*-dominated one is seen at c. 3.9 cal. ka BP. This shift is taken as illustrating a change from melt water influence, i.e. rather low salinities of c. 7 psu and therefore rather high water levels, to typical modern CS

waters with a salinity of 13 psu and therefore intermediate water levels. This change is seen in two cores, one from the centre of the south basin (core GS05) and one from the centre of the middle basin (core CP14) at 3.9 cal. ka (Leroy et al., 2007; Leroy, unpublished data; Fig. 1B). Clearly the shifts in assemblages do not have the same ages in the very shallow environments of Gomishan coast and offshore of it (Fig. 1C). In this sequence, the dinocyst change is not recorded and is assumed to have taken place before 10.6 cal. ka, if at all. The sediment in core TM displays thin evaporitic layers and mottling of the sediment at the transition between lithozones 5 and 6, i.e. a few hundreds of years before the radiocarbon date at 3545 cal. yr BP.

It is suggested that this hiatus corresponds to the major drop in salinity and in sea level seen at 3.9 cal. ka in the deep cores. From the point of view of the dinoflagellate assemblages, because of the differences between shallow waters and deep waters, the Neocaspian should therefore be regarded as a biozone and not a chronozone. In Iran around that time, the "Central Iranian Drought" period has been recognised in archaeological settlements (Schmidt et al., 2011).

6.3. Short delay in woodland expansion in the Early Holocene

In some diagrams of arid areas of SE Europe and SW Asia a delay in the expansion of trees at the beginning of the Holocene is observed; it lasted c. 3000 years in Lake Van in eastern Turkey (Wick et al., 2003), in Lake Urmia in N. Iran (Bottema, 1986), in Lake Zeribar in NW Iran (van Zeist and Bottema, 1977), in Lake Mirabad in W. Iran (van Zeist and Bottema, 1977) and finally c. 2500 years in core G05 in the middle of the south basin of the CS (Pierret et al., 2012); but the delay was only one millennium long in Aligol in the mountains of eastern Georgia (Connor, 2006).

Wright et al. (2003) suggest that an early Holocene dry period occurred from the Balkan Peninsula to southern Siberia when Europe had a climatic optimum. They propose that the cause is summer aridity (deficit of monsoon) due to high insolation. Djamali et al. (2010), based on a study on the Zagros and Anti-Taurus Mountains in W Iran and SE Turkey, suggest a delay of monsoon leading to insufficient spring rains.

A slight woodland expansion exists here too but covers less than a single millennium (Fig. 6). Also the presence of considerable loess deposits along the coast and in the foothills of the Alborz Mountains of the same age underlines the dryness of the climate (Kazancı et al., 2004; Frechen et al., 2009).

This small difference in the length of the delay, long for example in the deep core of the south basin and short in the Gomishan core, may be due to the proximity of the Alborz Mountains that must have formed a refugial area for trees during Last Glacial period. Climate models show that warm-loving trees may have found sufficiently good conditions to grow in the south-east corner of the CS (Leroy and Arpe, 2007; Arpe et al., 2011). The site in Georgia may have benefited in the same way from the proximity of glacial refugia according to the same modelling studies.

6.4. Vegetation succession

The present TM diagram contributes to the question of which succession was followed by trees when migrating out the glacial refugia in the Alborz Mountains (Leroy and Arpe, 2007; Arpe et al., 2011). These mountains contain relict Arcto-Tertiary thermophilous species such as *P. persica*, *G. caspica*, *Z. carpinifolia* and *P. fraxinifolia,* amongst which some had larger distributions in Europe during the Quaternary (Leroy and Roiron, 1996; Akhani et al., 2010).

Here the succession is as follows: deciduous *Quercus, C. betulus, P. persica,* and *F. orientalis-P. fraxinifolia* (Fig. 6). The succession reconstructed from Georgia is rather different: first *Betula* and *Corylus*, then *Abies, Carpinus, Fagus, Quercus* and *Castanea* and finally *Picea, Pinus, Juglans* and *Ostrya*-t. (Connor and Kvavadze, 2008). A pollen diagram from a marine core taken offshore the Pontic Mountains influenced by the Euxinian forest shows the following succession of trees: deciduous *Quercus, Pinus-Abies* with some *Ephedra distachya*-t., *Alnus-Fagus-C. betulus-Corylus-Juniperus*, and finishes with the appearance of anthropogenic indicators (Shumilovskikh et al., 2012).

As no other Holocene diagrams with *P. persica*, a useful comparison can only be made with Early Pleistocene pollen diagrams of Western Europe, such as that of Nogaret, High Languedoc, Southern France (Leroy and Seret, 1992; Leroy et al., 1999), where a similar succession of taxa is indeed seen: deciduous *Quercus, Carpinus, P. persica, Carya-Picea, Tsuga-Pterocarya*. The main differences are 1) *Carya* that starts spreading in the middle of the interglacial and is now absent from Europe and western Asia and 2) the conifers which appear in the middle and last parts of the interglacial and whose plants do not grow in the Hyrcanian area. The climate of the southern coast of the Caspian Sea has been used as an analogue to that of Western Europe in the Early Pleistocene: milder winters, more rainfall and reduced seasonal contrast (Leroy and Roiron, 1996).

6.5. The Pterocarya decline and the Sasanian Empire

A well-defined *Pterocarya* decline occurs in diagrams in Northern Iran and in western Georgia (Kvavadze, 1982 in Connor, 2006; Connor et al., 2007; Ramezani et al., 2008; de Klerk et al., 2009; Akhani et al., 2010). This takes place at ages ranging from around AD 780–1350. The decline has been variously attributed to a regional climatic drying, *P. fraxinifolia* being a tree of humid soils, and to human activities. Native people use the leaf of this tree as an anaesthetic agent for catching fish, for dyeing and as an antifungal agent (Hadjmohammadi and Kamel, 2006). Its nut is edible. Its wood however is of little use in joinery.

In core TM, this decline is seen at the transition pz TM-7a/b at around AD 495 (Fig. 6); therefore it occurs earlier than further west. The decline of *Pterocarya* in the studied region corresponds to the time when the Sasanian Empire in the early Middle Ages built the Gorgan wall and associated buildings. Human interference in the demise of the *Pterocarya* cannot be ruled out in addition to the aridification of the climate.

An east–west trend may also exist with an earlier decline of *Pterocarya* in the drier east than in the wetter west. The region of study is close to the easternmost limit of the species distribution at present (Browicz, 1982). Although the pollen of this tree is abundant in the surface samples (mud and moss) of Nahar Khoran near Gorgan town, it is absent from the surface samples 190 km further east of Gorgan in the Golestan National Park (Djamali et al., 2009). This proximity to the species distribution limits may make it more sensitive to anthropogenic or climatic changes.

6.6. End of the lagoon and afforestation

Historical Landsat satellite imagery of 1975 indicates that the location of core TM was already dry. The top sample of the TM pollen diagram, i.e. at 20 cm depth, already has rather high values of AP, i.e. 40%, due to the post-1972 afforestation (Fig. 4). Therefore this would suggest that the sediment of pz TM-8 is younger than 1972 and that sediment was still accumulating there at that time.

The recent afforestation is not felt in the recent sequences of Amirkola, Anzali and Muzidarbon, further west on the coast and in areas that have remained more closely forested despite human influence (Ramezani et al., 2008; Leroy et al., 2011), which is likely

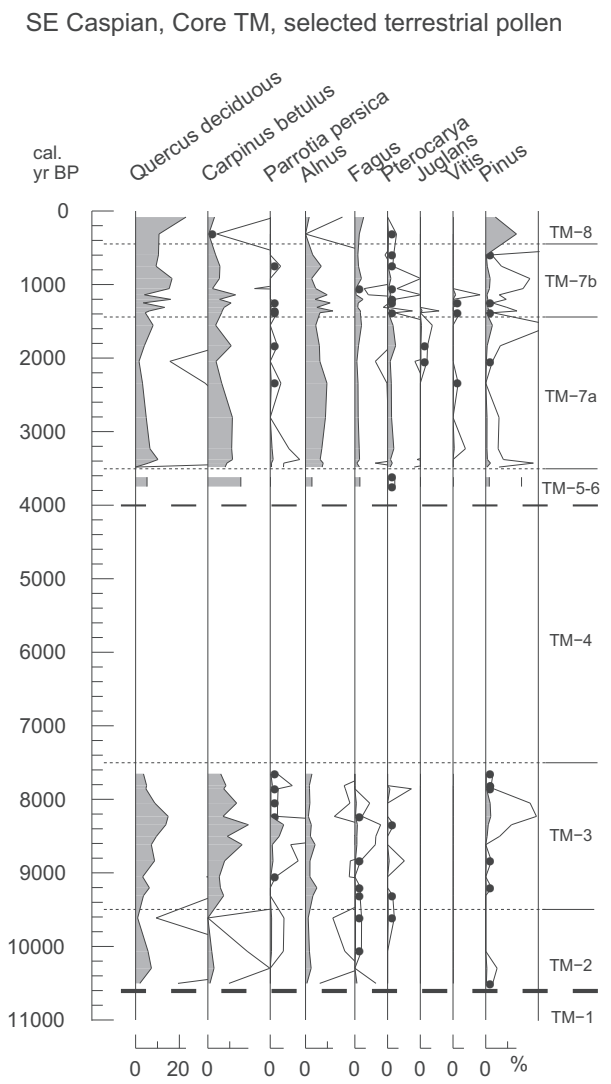

Fig. 6. Selected terrestrial pollen from the diagram of core TM, Gomishan, plotted against time.

because the environment at the location of core TM is very open and therefore records better the pollen rain derived from more or less distant plantations.

7. Conclusions

The palynological investigation of the 27.7 m long core TM, near the lagoon of Gomishan in the south-east corner of the CS, has provided novel and significant results regarding vegetation history and sea level changes.

The delay in woodland expansion at the beginning of the Holocene, which is typical of eastern Turkey, the Iranian plateau, and that was also recorded in the south CS basin, is only weakly felt at the north-eastern foothill of the Alborz Mountains, as Gomishan is close to postulated glacial refugia of trees. The succession of the main trees out of their refugia has been established as deciduous *Quercus, C. betulus, P. persica,* and *F. orientalis-P. fraxinifolia*, presenting therefore close affinities to south European interglacials in the Early Pleistocene. A *Pterocarya* decline is observed at AD 495. The region, close to the easternmost tree distribution, has been affected earlier than elsewhere in the northern Alborz and the Caucasus where similar declines were observed, perhaps due to human activities during the Sasanian Empire and the subsequent drying of the climate.

After a Late Pleistocene/Early Holocene lowstand, a maximum sea level occurs in the first part of the Holocene from 10.6 to 7.2 cal. ka. It is suggested that an inflow from the Uzboy (via the Amu-Daria) brought waters from the Pamir and Tien-Shan glaciers that were well developed at that time owing to a strong summer monsoon. The monsoonal regime therefore had a significant contribution to the CSL. A period of low level follows between 7.3 and 3.5 cal. ka, with a minimum at 3.9 cal. ka. From 3.5 cal. ka to the present, a series of small fluctuations took place. Finally, it is recommended that the Neocaspian period following the Mangyshlak period, a lowstand marked here by a major hiatus, should be considered a biozone rather than a chronozone. Indeed the environmental conditions reconstructed from dinocyst assemblages are different in shallow shelf waters from those in the deep basins of the CS, with an earlier assemblage shift on the shelf than in the deep basins.

Acknowledgements

Our gratitude goes to the numerous people who have assisted in taking the modern samples. We are grateful to Dr H. A. Nasrollahzadeh (Caspian Sea Ecology Research Centre) for the grab samples offshore of Babolsar and Bandar-e-Torkmen. Dr A. Naqinezhad (University of Mazandaran) provided the information on the distribution of *Alnus subcordata*. This article is a contribution to the European project Marie Curie, CLIMSEAS-PIRSES-GA-2009-247512: "Climate Change and Inland Seas: Phenomena, Feedback and Uncertainties. The Physical Science Basis". Thank you to Dr K. Arpe (Max Plank Institute of Meteorology and Brunel University) who prepared the map of Fig. 1A, to Mr O. Guchgeldiyev (Environmental and Local Development Consultant) for translations from Russian and to Dr F. Marret (University of Liverpool) who constructively reviewed the manuscript. Mr M. Turner (Brunel University) has kindly revised the English of the manuscript.

References

Akhani, H., Djamali, M., Ghorbanalizadeh, A., Ramezani, E., 2010. Plant biodiversity of Hyrcanian relict forests, N Iran: an overview of the flora, vegetation, palaeoecology and conservation. Pakistan Journal of Botany 42, 231–258.

Arpe, K., Leroy, S.A.G., Lahijani, H., Khan, V., 2012. Impact of the European Russia drought in 2010 on the Caspian Sea level. Hydrology and Earth System Sciences 16, 19–27.

Arpe, K., Leroy, S.A.G., Mikolajewicz, U., 2011. A comparison of climate simulations for the Last Glacial maximum with three different versions of the ECHAM model and implications for summer-green tree refugia. Climate of the Past 7, 91–114.

Bennett, K., 2007. Documentation for Psimpoll and Pscomb. http://www.chrono.qub.ac.uk/psimpoll/psimpoll.html, Last accessed on 28 Feb. 2012.

Boomer, I., von Grafenstein, U., Guichard, F., Bieda, S., 2005. Modern and Holocene sublittoral ostracod assemblages (Crustacea) from the Caspian Sea: a unique brackish, deep-water environment. Palaeogeography, Palaeoclimatology, Palaeoecology 225, 173–186.

Bottema, S., 1986. A late Quaternary pollen diagram from Lake Urmia (northwestern Iran). Review of Palaeobotany and Palynology 47, 241–261.

Bottema, S., Barkoudah, Y., 1979. Modern pollen precipitation in Syria and Lebanon and its relationship to vegetation. Pollen and Spores 21 (4), 427–480.

Browicz, K., 1982. Chorology of Trees and Shrubs in SW Asia and Adjacent Regions. Polish Academy of Sciences, Polish Scientific Publishers, Warszawa-Poznan.

Chen, F.H., Yu, Z.C., Yang, M.L., Ito, E., Wang, S.M., Madsen, D.B., Huang, X.Z., Zhao, Y., Sato, T., Birks, H.J.B., Boomer, I., Chen, J.H., An, C.B., Wünnemann, B., 2008. Holocene moisture evolution in arid central Asia and its out-of-phase relationship with Asian monsoon history. Quaternary Science Reviews 27, 3–4, 351–364.

Connor, S.E., 2006. A Promethean Legacy: Late Quaternary Vegetation History of Southern Georgia, Caucasus. PhD thesis. University of Melbourne, Australia.

Connor, S.E., Thomas, I., Kvavadze, E.V., 2007. A 5600-yr history of changing vegetation, sea levels and human impacts from the Black Sea coast of Georgia. The Holocene 17, 25–36.

Connor, S.E., Kvavadze, E.V., 2008. Modelling late Quaternary changes in plant distribution, vegetation and climate using pollen data from Georgia, Caucasus. Journal of Biogeography 36, 529–545.

de Klerk, P., Haberl, A., Kaffke, A., Krebs, M., Matchutadze, I., Minke, M., Schulz, J., Joosten, H., 2009. Vegetation history and environmental development since ca. 6000 cal yr BP in and around Ispani 2 (Kolkheti lowlands, Georgia). Quaternary Science Reviews 28, 890–910.

Djamali, M., de Beaulieu, J.-L., Campagne, P., Akhani, H., Andrieu-Ponel, V., Ponel, P., Leroy, S., 2009. Modern pollen rain-vegetation relationships along a forest-steppe transect in the Golestan National Park, N-E Iran. Review of Palaeobotany and Palynology 153, 3–4, 272–281.

Djamali, M., de Beaulieu, J.-L., Campagne, P., Andrieu-Ponel, V., Ponel, P., Cheikh Albassatneh, M., Leroy, S., 2008. Pollen rain-vegetation relationships along a forest-steppe transect in Golestan National Park, NE Iran. Ecologia Mediterranea 34, 35–52.

Djamali, M., Andrieu-Ponel, V., Ponel, P., de Beaulieu, J.L., Braconnot, P., Lézine, A.-M., Médail, F., Akhani, H., Fleitmann, D., Fleury, J., Gasse, F., Roberts, N., Stevens, L., 2010. Indian summer monsoon variations could have affected the early Holocene woodland expansion in the Near East. Holocene 20, 813–820.

Encyclopaedia Iranica, no date. http://www.iranicaonline.org/articles/alborz-massif-iran#pt3. Last accessed 1 March 2012.

Ferronsky, V.I., Polyakov, V.A., Kuprin, P.N., Lobov, A.L., 1999. The nature of variations in the level of the Caspian Sea (based on bottom sediment data). Water Resources 26 (6), 583–596.

Frechen, M., Kehl, M., Rolf, C., Sarvati, R., Skowronek, A., 2009. Loess chronology of the Caspian Lowland in Northern Iran. Quaternary International 198, 220–233.

Gasse, F., Fontes, J.Ch., Van Campo, E., Wei, K., 1996. Holocene environmental changes in Bangong Co basin (Western Tibet). Part 4: discussion and conclusions. Palaeogeography, Palaeoclimatology, Palaeoecology 120, 79–92.

Giralt, S., Julià, R., Klerkx, J., Riera, S., Leroy, S., Buchaca, T., Catalan, J., De Batist, M., Beck, C., Bobrov, V., Gavshin, V., Kalugin, I., Sukhorukov, F., Brennwald, M., Kipfer, R., Peeters, F., Lombardi, S., Matychenkov, V., Romanovsky, V., Podsetchine, V., Voltattorni, N., 2004. 1,000 year environmental history of Lake Issyk-Kul. In: Nihoul, J., Zavialov, P., Micklin, P. (Eds.), Dying and Dead Seas, Climatic versus Anthropic Causes. NATO ASI Series, vol. 36. Kluwer Academic Publishers, pp. 253–285.

Goodbred, S.L., Kuehl, S.A., 2000. Enormous Ganges–Brahmaputra sediment discharge during strengthened early Holocene monsoon. Geology 28 (12), 1083–1086.

Hadjmohammadi, M.R., Kamel, K., 2006. Determination of Juglone (5-hydroxy 1,4-naphthoquinone) in *Pterocarya fraxinifolia* by RP-HPLC. Iranian Journal of Chemistry & Chemical Engineering 25 (4), 73–76.

Honardoust, F., Ownegh, M., Sheikh, V., 2011. Assessing desertification sensitivity in the northern part of Gorgan Plain, southeast of the Caspian Sea, Iran. Research Journal of Environmental Sciences 5 (3), 205–220.

Horowitz, A., 1992. Palynology of Arid Lands. Elsevier Science, Amsterdam–London–New York–Tokyo.

Jamshidi, S., Bin Abu Bakar, N., 2011. Oceanographic study in coastal waters of Babolsar. Asian Journal of Earth Sciences 4 (1), 1–8.

Kakroodi, A.A., 2012. Rapid Caspian Sea-level Change and Its Impact on Iranian Coast. Doctoral thesis. Delft University of Technology.

Kakroodi, A.A., Kroonenberg, S.B., Hoogendoorn, R.M., Mohammed Khani, H., Yamani, M., Ghassemi, M.R., Lahijani, H.A.K., 2012. Rapid Holocene sea-level changes along the Iranian Caspian coast. Quaternary International 263, 93–103.

Karimi, Z., 2010. Study of flora and vegetation of international Gomishan Lagoon. Iranian Journal of Biology 23 (3), 436–447.

Kvavadze, E.V., 1982. Novye dannye po stratigrafii i paleogeografii Golotsena Kolkhidskoi nizmennosti, Chetvertichnaia Sistema Gruzii. Metsniereba, Tbilisi, pp. 123–130.

Kazancı, N., Gulbabazadeh, T., Leroy, S.A.G., Ileri, O., 2004. Sedimentary and environmental characteristics of the Gilan-Mazenderan plain, northern Iran: influence of long- and short-term Caspian water level fluctuations on geomorphology. Journal of Marine Systems 46 (1–4), 145–168.

Kuprin, P.N., Ferronsky, V.I., Popovchak, V.P., Shlykov, V.G., Zolotaya, L.A., Kalisheva, M.V., 2003. Bottom sediments of the Caspian Sea as an indicator of changes in its water regime. Water Resources 30 (2), 136–153.

Lahijani, H.A.K., Tavakoli, V., Amini, A.H., 2008. South Caspian river mouth configuration under human impact and sea level fluctuations. Environmental Sciences 5 (2), 65–86.

Leroy, S.A.G., 2010. Palaeoenvironmental and palaeoclimatic changes in the Caspian Sea region since the Lateglacial from palynological analyses of marine sediment cores. Geography, Environment, Sustainability, Faculty of Geography of Lomonosov Moscow State University and by the Institute of Geography of RAS 2, 32–41.

Leroy, S.A.G., Arpe, K., 2007. Glacial refugia for summer-green trees in Europe and S-W Asia as proposed by ECHAM3 time-slice atmospheric model simulations. Journal of Biogeography 34, 2115–2128.

Leroy, S.A.G., Boyraz, S., Gürbüz, A., 2009. High-resolution palynological analysis in Lake Sapanca as a tool to detect earthquakes on the North Anatolian Fault. Quaternary Science Reviews 28, 2616–2632.

Leroy, S.A.G., Lahijani, H.A.K., Djamali, M., Naqinezhad, A., Moghadam, M.V., Arpe, K., Shah-Hosseini, M., Hosseindoust, M., Miller, Ch.S., Tavakoli, V., Habibi, P., Naderi, M., 2011. Late Little Ice Age palaeoenvironmental records from the Anzali and Amirkola lagoons (south Caspian Sea): vegetation and sea level changes. Palaeogeography, Palaeoclimatology, Palaeoecology 302, 415–434.

Leroy, S.A.G., Marret, F., Gibert, E., Chalié, F., Reyss, J.-L., Arpe, K., 2007. River inflow and salinity changes in the Caspian Sea during the last 5500 years. Quaternary Science Reviews 26, 3359–3383.

Leroy, S.A.G., Marret, F., Giralt, S., Bulatov, S.A., 2006. Natural and anthropogenic rapid changes in the Kara-Bogaz Gol over the last two centuries by palynological analyses. Quaternary International 150, 52–70.

Leroy, S.A.G., Roiron, P., 1996. Final Pliocene macro and micro floras of the paleovalley of Bernasso (Escandorgue, France). Review of Palaeobotany and Palynology 94, 295–328.

Leroy, S., Seret, G., 1992. Duration and vegetation dynamic of the Nogaret Interglacial (1.9 Ma, S. France). Tentative correlation with stage 75. In: Kukla, G., Went, E. (Eds.), Start of a Glacial. Proceedings of the Mallorca NATO ARW, NATO ASI Series I, vol. 3. Springer Verlag, Heidelberg, pp. 113–125.

Leroy, S., Wrenn, J., Suc, J.-P., 1999. Global setting to comparative charts of regional events. In: Wrenn, J., Leroy, S., Suc, J.-P. (Eds.), The Pliocene: Time of Change. Amer. Ass. Stratigr. Palynologists Series, Contr. Series, pp. 1–12.

Létolle, R., 2000. Histoire de l'Ouzboï, cours fossile de l'Amou Darya synthèse et éléments nouveaux. Studia Iranica 29 (2), 195–240.

Marret, F., Leroy, S., Chalié, F., Gasse, F., 2004. New organic-walled dinoflagellate cysts from recent sediments of central Asian seas. Review of Palaeobotany and Palynology 129, 1–20.

McCarthy, F.M.G., Mudie, P.J., 1998. Oceanic pollen transport and pollen: dinocyst ratios as markers of late Cenozoic sea level change and sediment transport. Palaeogeography, Palaeoclimatology, Palaeoecology 138, 187–206.

Mertens, K.N., Ribeiro, S., Bouimetarhan, I., Caner, H., Combourieu-Nebout, N., Dale, B., de Vernal, A., Ellegaard, M., Filipova, M., Godhe, A., Grøsfjeld, K., Holzwarth, U., Kotthoff, U., Leroy, S., Londeix, L., Marret, F., Matsuoka, K., Mudie, P., Naudts, L., Peña-manjarrez, J., Persson, A., Popescu, S., Sangiorgi, F., van derMeer, M., Vink, A., Zonneveld, K., Vercauteren, D., Vlassenbroeck, J., Louwye, S., 2009. Process length variation in cysts of a dinoflagellate, *Lingulodinium machaerophorum*, in surface sediments investigating its potential as salinity proxy. Marine Micropaleontology 70, 54–69.

Mudie, P.J., Leroy, S.A.G., Marret, F., Gerasimenko, N., Kholeif, S.E.A., Sapelko, T., Filipova-Marinova, M., 2011. Non-pollen palynomorphs: indicators of salinity and environmental change in the Caspian-Black Sea-Mediterranean corridor. In: Buynevich, I., Yanko-Hombach, V., Gilbert, A.S., Martin, R.E. (Eds.), Geology and Geoarchaeology of the Black Sea Region: Beyond the Flood Hypothesis. Geological Society of America Special Paper 473, pp. 89–115.

Nokandeh, J., Sauer, E.W., Omrani Rekavandi, H., Wilkinson, T., Abbasi, G.A., Schwenninger, J.-L., Mahmoudi, M., Parker, D., Fattahi, M., Usher-Wilson, L.S., Ershadi, M., Ratcliffe, J., Gale, R., 2006. Linear barriers of northern Iran: The Great Wall of Gorgan and the Wall of Tammishe. Iran 44, 121–173.

Omrani Rekavandi, H., Sauer, E., Wilkinson, T., Nokandeh, J., 2008. The enigma of the "Red Snake". Current World Archaeology 27, 12–22.

Owen, L.A., Finkel, R.C., Barnard, P.L., Haizhou, M., Asahi, K., Caffee, M.W., Derbyshire, E., 2005. Climatic and topographic controls on the style and timing of Late Quaternary glaciation throughout Tibet and the Himalaya defined by ^{10}Be cosmogenic radionuclide surface exposure dating. Quaternary Science Reviews 24, 1391–1411.

Patimar, R., 2008. Fish species diversity in the lakes of Alma-Gol, Adji-Gol, and Ala-Gol, Golestan Province, northern Iran. Journal of Ichthyology 48 (10), 911–917.

Patimar, E., Yousefi, M., Hoseini, S.M., 2009. Age, growth and reproduction of the sand smelt *Atherina boyeri* Risso, 1810 in the Gomishan wetland – southeast Caspian Sea. Estuarine, Coastal and Shelf Science 81, 457–462.

Peterson, G.M., 1983. Recent pollen spectra and zonal vegetation in the western USSR. Quaternary Science Reviews 2, 281–321.

Pierret, M.C., Chabaux, F., Leroy, S.A.G., Causse, C., 2012. A record of Late Quaternary continental weathering in the sediment of the Caspian Sea: evidence from U-Th, Sr isotopes, trace element and palynological data. Quaternary Science Reviews 51, 40–55.

Ramezani, E., Joosten, H., Mohadjer, M.R.M., Knapp, H.-D., Ahmadi, H., 2008. The late-Holocene vegetation history of the Central Caspian (Hyrcanian) forests of northern Iran. The Holocene 18 (2), 305–319.

Reimer, P.J., Baillie, M.G.L., Bard, E., Bayliss, A., Beck, J.W., Blackwell, P.G., Bronk Ramsey, C., Buck, C.E., Burr, G.S., Edwards, R.L., Friedrich, M., Grootes, P.M., Guilderson, T.P., Hajdas, I., Heaton, T.J., Hogg, A.G., Hughen, K.A., Kaiser, K.F., Kromer, B., McCormac, F.G., Manning, S.W., Reimer, R.W., Richards, D.A., Southon, J.R., Talamo, S., Turney, C.S.M., van der Plicht, J., Weyhenmeyer, C.E., 2009. IntCal09 and marine09 radiocarbon age calibration curves, 0–50,000 years cal BP. Radiocarbon 51 (4), 1111–1150.

Rekacewicz, P., 2007a. http://www.grida.no/graphicslib/detail/caspian-sea-salinity_829b, last accessed 28 Feb. 2012.

Rekacewicz, P., 2007b. http://www.grida.no/graphicslib/detail/mean-sea-surface-temperature-on-the-caspian-sea_167e, last accessed 28 Feb. 2012.

Rychagov, G.I., 1997. Holocene oscillations of the Caspian Sea, and forecasts based on palaeogeographical reconstructions. Quaternary International 41/42, 167–172.

Sagheb-Talebi, K., 2004. Rehabilitation of temperate forests in Iran (Chapter 26). In: Stanturf, J.A., Madsen, P. (Eds.), Restoration of Boreal and Temperate Forests. CRC Press, New York, pp. 397–407.

Schmidt, A., Quigley, M., Fattahi, M., Azizi, G., Maghsoudi, M., Fazeli, H., 2011. Holocene settlement shifts and palaeoenvironments on the Central Iranian Plateau: investigating linked systems. The Holocene 21 (4), 583–595.

Shumilovskikh, L., Tarasov, P., Arz, H.W., Fleitmann, D., Marret, F., Nowaczyk, N., Plessen, B., Schlütz, F., Behling, H., 2012. Vegetation and environmental dynamics in the southern Black Sea region since 18 kyr BP derived from the marine core 22-GC3. Palaeogeography, Palaeoclimatology, Palaeoecology 337-338, 177–193.

Svitoch, A.A., 2009. Khvalinian transgression of the Caspian Sea was not the result of water overflow from the Siberian Proglacial lakes, nor a prototype of the Noachian flood. Quaternary International 197, 115–125.

Syrnyov, I.P., 1962. Uzboy, Its Relation to the Ancient Caspian. Collection of Materials of the Complex Geological Expedition. In: Structural-geomorphological Research in Near-Caspian, Issue 7, Leningrad. (In Russian).

van Zeist, W., Baruch, U., Bottema, S., 2009. Holocene palaeoecology of the Hula area, Northeastern Israel. In: Kaptijn, W., Lucas, P. (Eds.), A timeless Vale. Archaeological and Related Essays on the Jordan Valley in Honor of Gerrit van der Kooij on the Occation of his Sixty-fifth Birthday. Archaeological Studies Leiden University, vol. 19. Leiden University Press, pp. 29–64.

van Zeist, W., Bottema, S., 1977. Palynological investigations in western Iran. Palaeohistoria 19, 19–85.

Weinstein, A., 1989. Provenance evaluation of *Pinus halepensis, P. brutia* and *P. eldarica* in Israel. Forest Ecology and Management 26, 215–225.

Wick, L., Lemke, G., Sturm, M., 2003. Evidence of Lateglacial and Holocene climatic change and human impact in eastern Anatolia: high resolution pollen, charcoal, isotopic and geochemical records from the laminated sediments of Lake Van, Turkey. The Holocene 13, 665–675.

Wright, H.E., Ammann, B., Stefanova, I., Atanassova, J., Margalitadze, N., Wick, L., Blyakharchuk, T., 2003. Late-Glacial and Early-Holocene dry climates from the Balkan Peninsula to southern Siberia. In: Tonkov, S. (Ed.), Aspects of Palynology and Palaeoecology: Festschrift in Honour of Elissaveta Bozilova. Pensoft, Sofia, pp. 127–136.

Wünnemann, B., Demske, D., Tarasov, P., Kotlia, B.S., Reinhardt, C., Bloemendal, J., Diekmann, B., Hartmann, K., Krois, J., Riedel, R., Arya, N., 2010. Hydrological evolution during the last 15 kyr in the Tso Kar lake basin (Ladakh, India), derived from geomorphological, sedimentological and palynological records. Quaternary Science Reviews 29 (9–10), 1138–1155.